Title:

Low doses of the organic insecticide spinosad trigger lysosomal defects, ROS driven lipid dysregulation and neurodegeneration in flies

Author names and affiliations:

Felipe Martelli[1,6], Zuo Zhongyuan[2], Julia Wang[2,7], Ching-On Wong[3,8], Nicholas E. Karagas[3], Ute Roessner[1], Thusitha Rupasinghe[1], Kartik Venkatachalam[3], Trent Perry[1], Philip Batterham[1*†], Hugo J. Bellen[2,4,5,*†]

[1]School of BioSciences, The University of Melbourne, Melbourne, VIC 3052, Australia
[2]Department of Molecular and Human Genetics, Baylor College of Medicine, Houston, TX 77030, USA
[3]Department of Integrative Biology and Pharmacology, McGovern Medical School at the University of Texas Health Sciences Center, Houston, TX 77030, USA
[4]Neurological Research Institute, Texas Children Hospital, Houston, TX 77030, USA
[5]Howard Hughes Medical Institute, Baylor College of Medicine, Houston, TX 77030, USA
[6]Present address: School of Biological Sciences, Monash University, Melbourne, VIC 3800, Australia
[7]Present address: Medical Scientist Training Program, Baylor College of Medicine, Houston, TX 77030, USA
[8]Present address: Department of Biological Sciences, Rutgers University, Newark, NJ 07102, USA

*Authors with equal contribution

Corresponding authors e-mail addresses
[†]Correspondence to: hbellen@bcm.edu and p.batterham@unimelb.edu.au

Keywords:
Spinosad, organic insecticide, oxidative stress, lipid dysregulation, neurodegeneration, antioxidant, lysosomal dysfunction.

Abstract

The plight of insect populations around the world and the threats it poses to agriculture and ecosystems has thrown insecticide use into the spotlight. Spinosad is an organic insecticide, considered less harmful to beneficial insects than synthetic insecticides, but its mode of action remains unclear. Using Drosophila, we show that low doses of spinosad reduce cholinergic response in neurons by antagonizing Dα6 nAChRs. Dα6 nAChRs are transported to lysosomes that become enlarged and accumulate upon spinosad treatment. Oxidative stress is initiated in the central nervous system, and spreads to midgut and disturbs lipid storage in metabolic tissues in a Dα6-dependent manner. Spinosad toxicity was ameliorated with the antioxidant N-Acetylcysteine amide (NACA). Chronic exposures lead to mitochondrial defects, severe neurodegeneration and blindness in adult animals. The many deleterious effects of low doses of this insecticide reported here point to an urgent need for rigorous investigation of its impacts on beneficial insects.

Introduction

The life-cycles of many plant species require pollination by insects, particularly bee species; 75% of crop plants depend on these pollination services to some extent (Klein et al., 2007). Every crop plant species faces the threat of attack by insect pests, typically countered using insecticides targeting proteins that are highly conserved among insect species (Sattelle et al., 2005). While insecticides maximise crop yield, they have the potential to negatively impact populations of insects that provide vital services in agriculture and horticulture (Sánchez-Bayo and Wyckhuys, 2019). There has been a sharp focus on the impact of neonicotinoid insecticides on bees, both in the scientific literature and in public discourse, because of evidence that these chemicals may contribute to the colony collapse phenomenon (Lu et al. 2014; Lundin et al. 2015). Many other insect species are under threat. A recent meta-analysis found an average decline of approximately 9% in terrestrial insect abundance per decade, since 1925 (van Klink et al., 2020), although estimates differ depending on the regions studied and the methodologies used (Wagner et al., 2021). While the extent to which insecticides are involved remains undetermined, they have consistently been associated as a major factor, along with climate change, habitat loss, pathogens and parasites (Cardoso et al., 2020; Sánchez-Bayo and Wyckhuys, 2019; Wagner et al., 2021).

In assessing the risk posed by insecticides, it is important that the molecular and cellular events that unfold following the interaction between the insecticide and its target be understood. Many insecticides target ion channels in the nervous system. At the high doses used to kill pests these insecticides produce massive perturbations to the flux of ions in neurons, resulting in lethality (Perry and Batterham, 2018). But non-pest insects are likely to be exposed to lower doses and the downstream physiological processes that are triggered are poorly understood. In a recent study, low doses of the neonicotinoid imidacloprid were shown to stimulate a constitutive flux of calcium into neurons via the targeted ligand gated ion channels (nicotinic acetylcholine receptors – nAChRs) (Martelli et al., 2020). This causes an elevated level of ROS and oxidative stress which radiates from the brain to other tissues. Mitochondrial damage leads to a significant drop in energy levels, neurodegeneration and blindness (Martelli et al., 2020). Evidence of compromised immune function was also presented, supporting other studies (Chmiel et al., 2019). Many other synthetic insecticides are known to elevate the levels of ROS (Karami-Mohajeri and Abdollahi, 2011; Lukaszewicz-Hussain, 2010; Wang et al., 2016) and may precipitate similar downstream impacts. Given current concerns about synthetic insecticides, a detailed analysis of the molecular and cellular impacts of organic alternatives is warranted. Here we report such an analysis for an insecticide of the spinosyn class, spinosad.

Spinosad is an 85%:15% mixture of spinosyns A and D, natural fermentation products of the soil bacterium *Saccharopolyspora spinosa*. It occupies a small (3%), but growing share of the global insecticide market (Sparks et al. 2017). It is registered for use in more than 80 countries and applied to over 200 crops to control numerous pest insects (Biondi et al., 2012). Recommended dose rates vary greatly depending on the pest and crop, ranging from 96 parts per million (ppm) for Brassica crops to 480 ppm in apple fields (Biondi et al., 2012). Garden sprays containing spinosad as the active ingredient contain doses of up to 5000 ppm. Like other insecticides, the level of spinosad residues found in the field vary greatly depending on the formulation, the application mode and dose used, environmental conditions and proximity to the site of application. If protected from light spinosad shows a half-life of up to 200 days (Cleveland et al., 2002).

Spinosad is a hydrophobic compound belonging to a lipid class known as polyketide macrolactones. Studies using mutants, field-derived resistant strains and heterologous expression have shown that spinosad targets the highly conserved nAChR Dα6 subunit in *Drosophila melanogaster* and a range of other insect species (Perry et al., 2015, 2007; Watson, 2001). This subunit is not targeted by imidacloprid (Watson et al., 2010). The two insecticides differ in their mode of action. Imidacloprid is an agonist causing cation influx into neurons by binding to a site that overlaps with that normally occupied by the native ligand, acetylcholine (ACh) (Buckingham et al., 1997; Martelli et al., 2020; Perry et al., 2008). Spinosad is an allosteric modulator, binding to a site in the C terminal region of the protein (Puinean et al., 2013; Somers et al., 2015). Salgado (1998) measured nerve impulses in cockroaches with electromyograms and found an increased response to spinosad, concluding that spinosad promoted an excitatory motor neuron effect. Salgado and Saar (2004) found that spinosad allosterically activates non-desensitized nAChRs, but that small doses were also capable of antagonizing the desensitized nAChRs. It is currently accepted that spinosad causes an increased sensitivity to ACh in certain nAChRs and an enhanced response at some GABAergic synapses, causing involuntary muscle contractions, paralysis and death (Biondi et al., 2012; Perry et al., 2011; Salgado, 1998). A recent study (Nguyen et al., 2021) showed that both acute and chronic exposures to spinosad causes Dα6 protein levels in the larval brain to decrease. A rapid loss of Dα6 protein during acute exposure was blocked by inhibiting the proteasome system (Nguyen et al., 2021). As *Dα6* loss of function mutants are viable (Perry et al., 2007; Perry et al 2021), it was suggested that the toxicity of spinosad may be due to overloading of protein degradation pathways and/or the internalisation of spinosad where it may cause cellular damage. Spinosad has been shown to cause cellular damage via mitochondrial dysfunction, oxidative stress and programmed cell death in insect cells (*Spodoptera frugiperda* Sf9) (Xu et al., 2018; Yang et al., 2017).

Here we show that while spinosad by itself does not elicit Ca^{2+} flux in *Drosophila* neurons, the response elicited by the cholinergic agonist is stunted upon spinosad pretreatment. Following exposure to spinosad, Dα6 cholinergic receptors traffic to the lysosomes, which induces hallmarks of lysosomal dysfunction. We also show that oxidative stress stemming from lysosomal dysfunction, which is a key factor in spinosad's mode of action at low doses, triggers a cascade of damage that results in mitochondrial dysfunction, reduced energy levels, extensive neurodegeneration in the central brain and blindness. Given the high degree of conservation of the spinosad target between insect species (Perry et al., 2015), our data suggest that the potential for this insecticide to cause harm in other non-pest insects needs to be thoroughly investigated.

Results

Low doses of spinosad affect survival and prevent Ca^{2+} flux into neurons expressing *Dα6* nAChRs

As a starting point to study the systemic effects of low-dose spinosad exposure, a dose that would reduce the movement of third instar larvae by 50% during a 2 hr exposure was determined. This was achieved with a dose of 2.5 ppm (**Figure 1A**). 82% of exposed larvae placed back onto insecticide-free media after being rinsed did not undergo metamorphosis. Death occurred over the course of the next 8 days (**Figure 1B**). Of the 18% of larvae that underwent metamorphosis, only 4% emerged as adults. Pupae showed small and irregular morphology (**Figure 1C**). The effect of this dose was measured on primary culture of neurons expressing the spinosad target, the nAChR Dα6 subunit using the GCaMP5G:tdTomato cytosolic [Ca^{2+}] sensor. As no alterations in basal Ca^{2+} levels were detected in response to 2.5 ppm (**Figure 1D, E**), a dose of 25 ppm was tested, again with no measurable impact (**Figure 1D, E**). After 5 min of spinosad exposure, neurons were then stimulated by carbachol, a cholinergic agonist that activates nAChR. Spinosad-exposed neurons exhibited a significant decrease in cholinergic response when compared to non-exposed neurons (**Figure 1D, E**). Total Ca^{2+} content mobilized from ER remained unaltered as measured by thapsigargin-induced Ca^{2+} release (**Figure 1D, E**). These data suggest that spinosad blocks the function of Dα6-containing nAChRs.

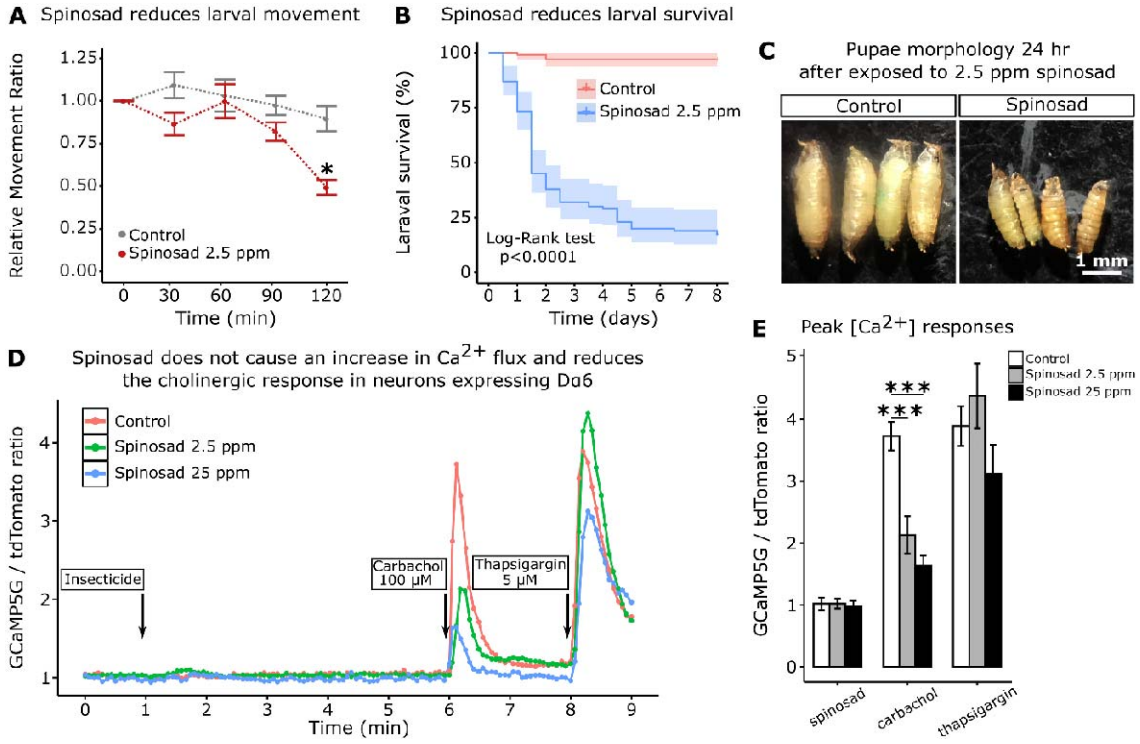

Figure 1. Low doses of spinosad are lethal and fail to increase Ca^{2+} levels in neurons. A, Dose response to spinosad by an assay of larval movement over time, expressed in terms of Relative Movement Ratio (RMR); n = 100 larvae/treatment). **B,** % Survival of larvae subjected to a 2 hr exposure to 2.5 ppm spinosad, rinsed and placed back onto insecticide-free medium (n = 100 larvae/treatment). **C,** Pupal morphology, 24 hr after exposure 2.5 ppm spinosad or control solution for 2 hr. **D,** Cytosolic [Ca^{2+}] measured by GCaMP in neurons expressing nAChR-Dα6. Measurement is expressed as a ratio of the signals of GCaMP5G signal and tdTomato. Spinosad (2.5 ppm or 25 ppm) was added to the bath solution at 1 minute after recording started. At 6 min and 8 min the spinosad and control groups were stimulated by 100 µM carbachol and 5 µM Thapsigargin, respectively. Each point represents the average of at least 50 cells. **E,** Peak [Ca^{2+}] responses to spinosad and carbachol. Error bars represent s.e.m.; shaded areas in **B** represent 95% confidence interval (Kaplan-Meier method and the Log-rank Mantel-Cox test; P < 0.0001). **A** and **E**, t-test; *P < 0.05, ***P <0.001.

Spinosad exposure causes lysosomal alterations, mitochondrial impairment and increase oxidative stress

To test whether blocked Dα6-containing nAChRs could cause receptor recycling from membrane and thus increase lysosome digestion, LysoTracker staining was used to assess lysosomal function. Whereas no phenotype was observed after 1 hr exposure, a 2 hr exposure to 2.5 ppm spinosad caused an 8-fold increase in the area occupied by lysosomes in the larval brain (**Figure 2A, B**). 6 hr after larvae were subjected to the 2 hr exposure, the area occupied by lysosomes in brains was 24-fold greater than in controls (**Figure 2A, B**). No increase in the area occupied by lysosomes was observed after exposure to imidacloprid, showing that this is a spinosad specific response (**Figure 2 – figure supplement 1**). These observations, in combination with the findings of Nguyen et al. (2021) suggested that binding of spinosad to Dα6 nAChRs may promote their trafficking to lysosomes. To investigate this hypothesis, the brains of larvae expressing a fluorescently (CFP) tagged Dα6 nAChR subunit were stained with LysoTracker. Exposure to 2.5 ppm spinosad showed a significant reduction of the Dα6 CFP signal from neuronal membranes over time and colocalization with lysosomes (**Figure 2C; Figure 2 – figure supplement 2**). Importantly, enlarged lysosomes were not observed in *Dα6 knockout* mutants, regardless of spinosad exposure (**Figure 2 – figure supplement 1**), indicating that the lysosomal expansion is dependent on the presence of Dα6 nAChRs.

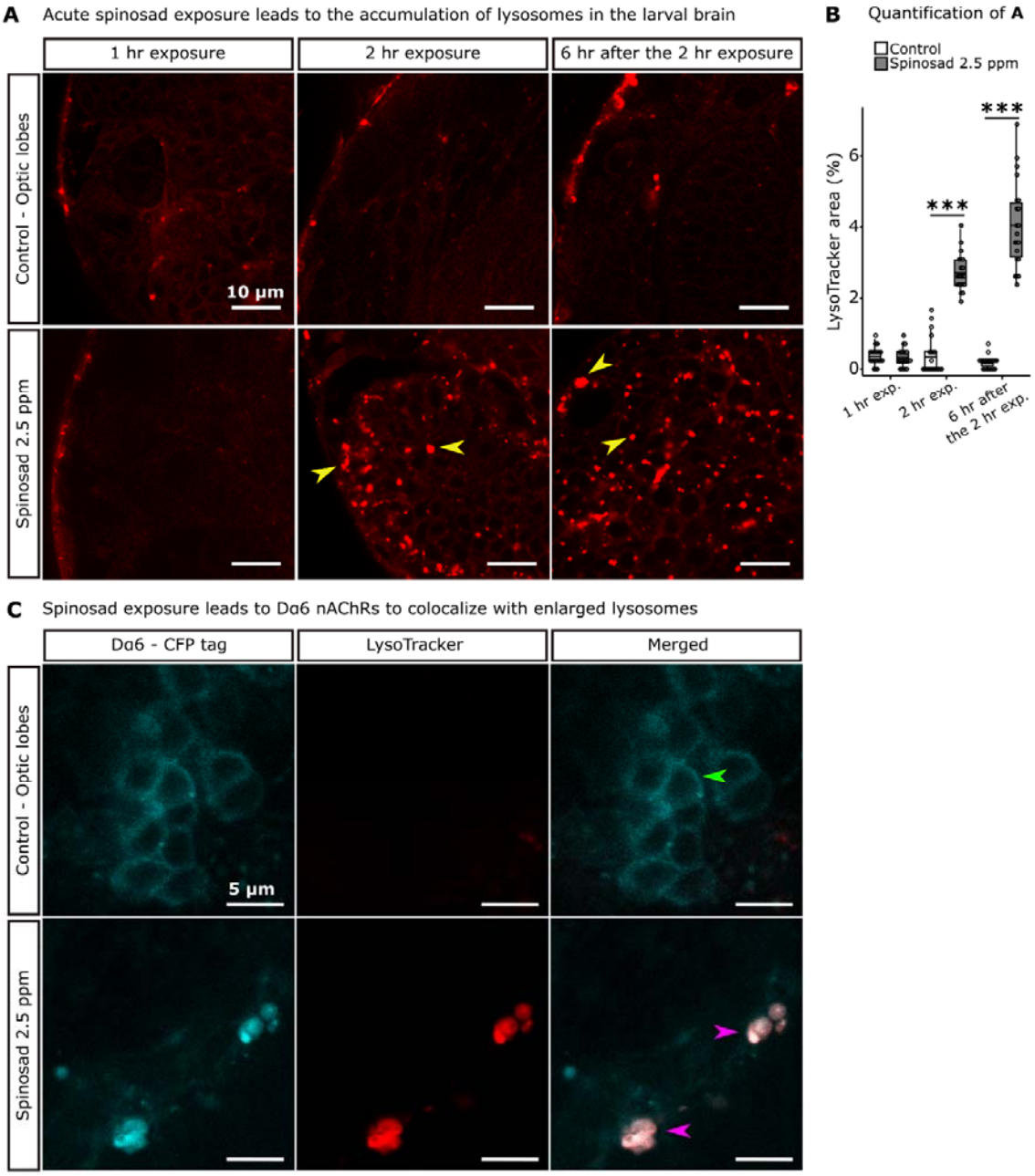

Figure 2. Spinosad exposure causes lysosomal expansion and Dα6 nAChRs colocalize with enlarged lysosomes. A, Larvae exposed to 2.5 ppm spinosad for 2hr show a significant increase in the number of enlarged lysosomes in the brain, not observed following a 1hr exposure. 6hrs after the 2hr exposure the number of enlarged lysosomes is further increased. Yellow arrowheads indicate enlarged lysosomes. Lysotracker staining, 400 x magnification. **B,** Lysotracker area in the optic lobes (%) (n = 7 larvae/treatment, 3 optic lobe sections/larva). **C,** Larvae expressing Dα6 tagged with CFP exposed to 2.5 ppm spinosad for 2 hr show co-localization of the Dα6 and lysosomal signals. Green arrowhead indicates Dα6 CFP signal in neuronal membranes of non-exposed larvae. Pink arrowheads indicate Dα6 CFP signal colocalizing with lysosomes. Lysotracker staining, 600 x magnification. Microscopy images obtained in Leica SP5 Laser Scanning Confocal Microscope. t-test; ***P < 0.001.

Defects in lysosomal function have been shown to impact other organelles, especially mitochondria (Deus et al., 2020). To assess mitochondrial dysfunction, we examined the levels of superoxide anion (O_2^-), a primary reactive oxygen species (ROS) produced by mitochondria (Valko et al., 2007), using dihydroethidium (DHE) staining. After a 1 hr exposure to 2.5 ppm spinosad, there was a mean 89% increase in O_2^- accumulation in the brain. After 2 hr the levels were lower than at the 1hr time point, but still 44% higher than in the unexposed controls (**Figure 3A, B**). A different pattern was observed in the anterior midgut. A significant increase in accumulation compared with the controls (28%) was only observed at the 2 hr time point (**Figure 3A, B**).

Mitochondrial turnover was assessed using the MitoTimer reporter line (Gottlieb and Stotland, 2015). A 2hr spinosad exposure induced an increase of 31% and 36% for the green (healthy mitochondria) and red (stressed mitochondria) signals in the optic lobes of the larval brain, respectively (**Figure 3C, D**). For the digestive tract, a 19% and 32% increase were observed in the proventriculus for green and red signal, respectively (**Figure 3C, D**). To examine the impact of ROS we measured the enzyme activity of mitochondrial aconitase, a highly ROS sensitive enzyme (Yan et al., 1997). We observed a mean 34% reduction in aconitase activity (**Figure 3E**), indicating an increased presence of ROS in mitochondria during the 2 hr exposure. Immediately after the 2 hr exposure, a mean 36% increase in systemic ATP levels was observed (**Figure 3F**), followed by a 16.5% reduction 12 hr after the 2 hr exposure (**Figure 3G**). The initial increase in energy levels is consistent with the increase in the green signal observed with MitoTimer at this time point. However, the reduction in ATP levels 12 hr after the exposure shows that the mitochondrial energy output is eventually impaired.

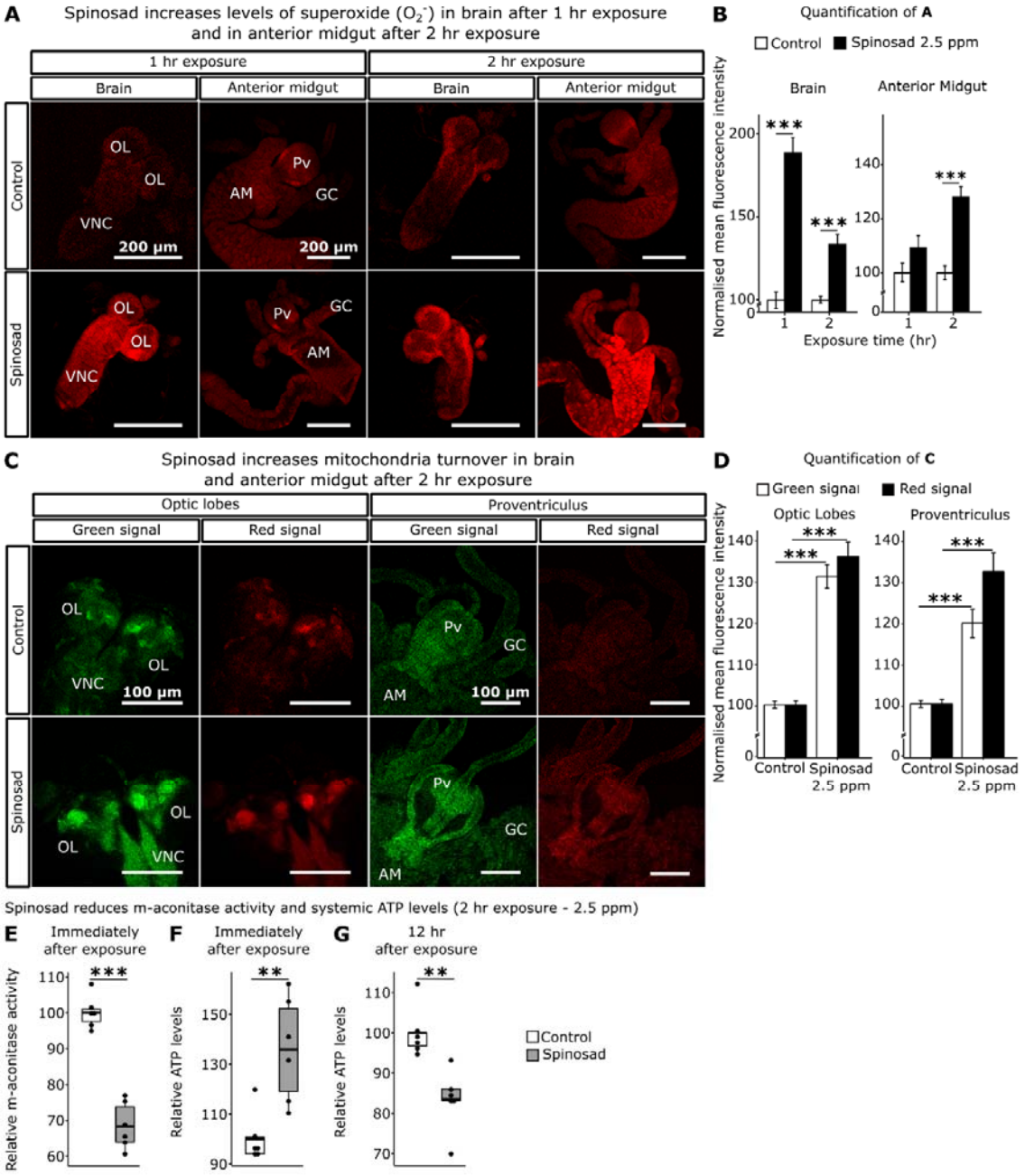

Figure 3. Spinosad exposure impacts ROS levels, mitochondrial turnover and energy levels. A, Superoxide levels in the brain and anterior midgut of larvae exposed to 2.5 ppm spinosad for either 1 hr or 2 hr. Tissue stained with DHE. **B,** Normalized mean fluorescence intensity of DHE (n = 15 larvae/treatment; 3 sections/larva). **C,** Optic lobes of the brain and proventriculus of MitoTimer reporter strain larvae. 2.5 ppm spinosad exposure for 2 hr increased the signal of healthy (green) and unhealthy (red) mitochondria (n = 20 larvae/treatment; 3 image sections/larva). **D,** Normalized mean fluorescence intensity of MitoTimer signals. Error bars indicate standard error. **E,** Relative m-aconitase activity in whole larvae (n = 25 larvae/replicate; 6 replicates/treatment) exposed to 2.5 ppm spinosad for 2 hr. **F,** Relative systemic ATP levels immediately after the 2 hr exposure to 2.5 ppm spinosad (n = 20 larvae/ replicate; 6 replicates/ treatment). **G,** Relative systemic ATP levels 12 hr after exposure to 2.5 ppm spinosad (n = 20 larvae/ replicate; 6 replicates/ treatment). OL – optic lobe; VNC – ventral nerve cord; Pv – proventriculus; GC – gastric caeca; AM – anterior midgut. Error bars in **B** and **D** represent mean ± s.e.m. Microscopy images obtained in Leica SP5 Laser Scanning Confocal Microscope, 200x magnification. t-test; **P < 0.01; ***P < 0.001.

Oxidative stress created by spinosad affects lipids, motility, and survival

Oxidative stress has the ability to affect the lipid environment of metabolic tissues, causing bulk redistribution of lipids into lipid droplets (LD) (Bailey et al., 2015). An elevation of ROS levels in the *Drosophila* larval brain has been shown to cause an increase in LD numbers in the fat body as well as a decreases LD in the midgut and Malpighian tubules (Martelli et al., 2020). The impact of spinosad on LD numbers was therefore examined. Larvae exposed to 2.5 ppm spinosad for 2 hr showed a 52% increase in the area covered by LD in the fat body (**Figure 4A, B**), with a significant reduction in the number of large LD and an increase in small LD (**Figure 4 – figure supplement 1**). Pre-treatment with the antioxidant N-Acetylcysteine amide (NACA) significantly reduced the impacts of spinosad exposure on this phenotype. Even though still significant, the area occupied by LD in fat bodies increased only 20% with NACA pre-treatment (**Figure 4A, B**). Antioxidant pre-treatment also significantly improved movement of larvae exposed to spinosad (**Figure 4C**), and survival, which increased from 4% to 15% (**Figure 4D**).

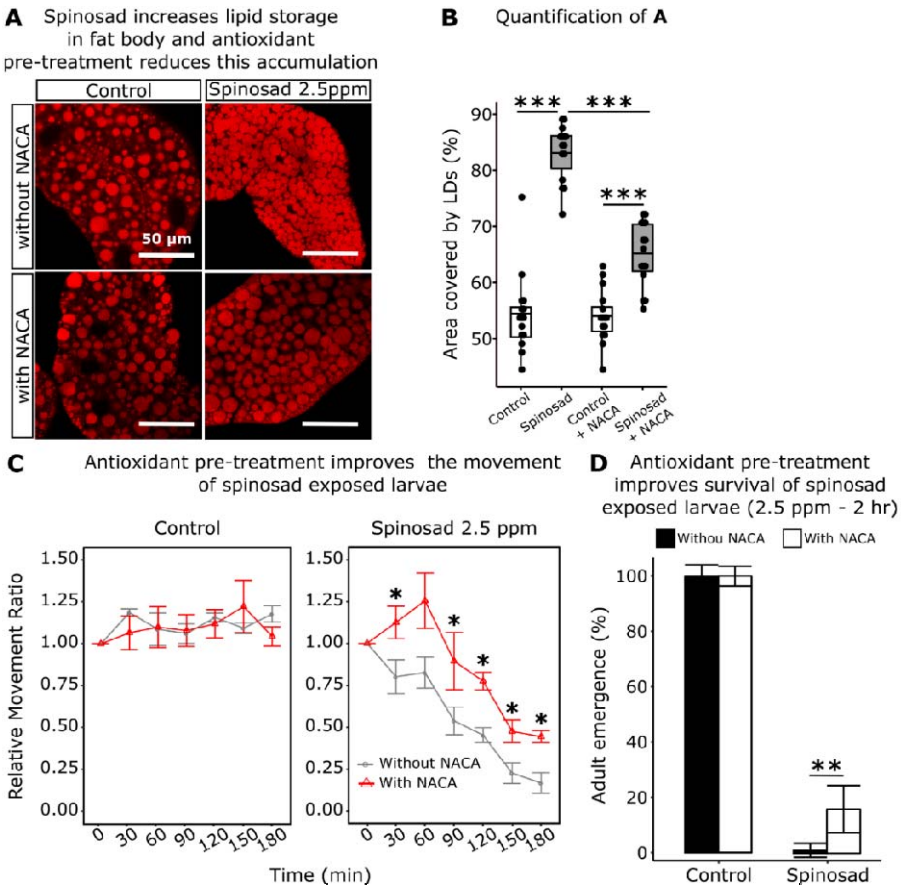

Figure 4. Spinosad increases lipid storage in fat body. Antioxidant pre-treatment reduces this accumulation and improves larval movement and survival. A, Larvae exposed to 2.5 ppm spinosad for 2 hr show an accumulation of LD in the fat body. A 5 hr pre-treatment with 300 µg/mL of antioxidant N-acetylcysteine amide (NACA) reduces this accumulation. Nile red staining. Images obtained using a Leica SP5 Laser Scanning Confocal Microscope, 400x magnification. **B,** Percentage of area occupied by LD in fat body (n = 3 larvae/treatment; 5 image sections/larva). **C,** Pre-treatment with NACA improves the movement of spinosad exposed larvae. Dose response to insecticide analysed using the Wiggle Index analysis. Results are expressed in terms of Relative Movement Ratio (RMR) values as a function of exposure time in minutes (n = 25 larvae/replicate; 4 replicates/ treatment). **D,** Pre-treatment with NACA improves survival of larvae exposed to spinosad. Corrected adult emergence (%) (n = 100 larvae/ treatment). Bars indicate corrected percentage survival (Abbots'

correction). Error bars in **C** represent the s.e.m. and in **D** the 95% confidence interval. t-test; *P < 0.05; **P < 0.01; ***P < 0.001.

In order to test whether doses that do not impact survival could also cause similar perturbations to the lipid environment, sublethal acute doses were determined. Larvae exposed to 0.5 ppm for 2 hr or 0.1 ppm for 4 hr showed no impact in adult eclosion after being rinsed and placed back onto insecticide-free media (**Figure 4 – figure supplement 2**). Both doses caused on average a 29% increase in the area occupied by LD in fat bodies (**Figure 4 – figure supplement 2**). That this impact is smaller than that observed for the 2.5 ppm shows that this phenotype is dose dependent. Once again, an increase in the number of small LD and reduction in the number of large LD was observed (**Figure 4 – figure supplement 3**). Using these sublethal doses, other metabolic tissues were investigated. The doses of 0.5 ppm for 2 hr and 0.1 ppm for 4 hr caused a mean 72% and 73% reduction in the total number of LD in the Malpighian tubules, respectively (**Figure 4 – figure supplement 2**). We also identified a reduction in the numbers of LD in the LD region of the posterior midgut (**Figure 4 – figure supplement 4**).

A brain signal triggers the impacts of spinosad on metabolic tissues

Once inside the insect body, spinosad could theoretically access any tissue via the open circulatory system. Given that the target Dα6 nAChRs are localized in the brain (Perry et al., 2015; Somers et al., 2015), and that elevated levels of ROS were observed earlier in the brain than in metabolic tissues, prompts a significant question. Could the interaction between spinosad and Dα6 in the brain provide the signal that ultimately leads to the observed disturbance of the lipid environment in the metabolic tissues? Two different *Dα6 knockout* mutants (Line 14 *Dα6 KO* and Canton S *Dα6 KO*) and their respective genetic background control lines (Line 14 – used in experiments so far, and Canton S) were tested. Larvae were exposed to 2.5 ppm of spinosad for 2 hr. Neither of the mutants tested showed an increase in the area occupied by LD, compared to their respective background lines, under conditions of spinosad exposure (**Figure 5A-D**). We also quantified the level of lipids in hemolymph. Whereas Line 14 and Canton S showed an average 10% and 13% increase in response to spinosad, respectively, neither of the *Dα6 KO* mutants showed significant changes (**Figure 5E**). Hence, *Dα6* mediates the observed lipid phenotypes.

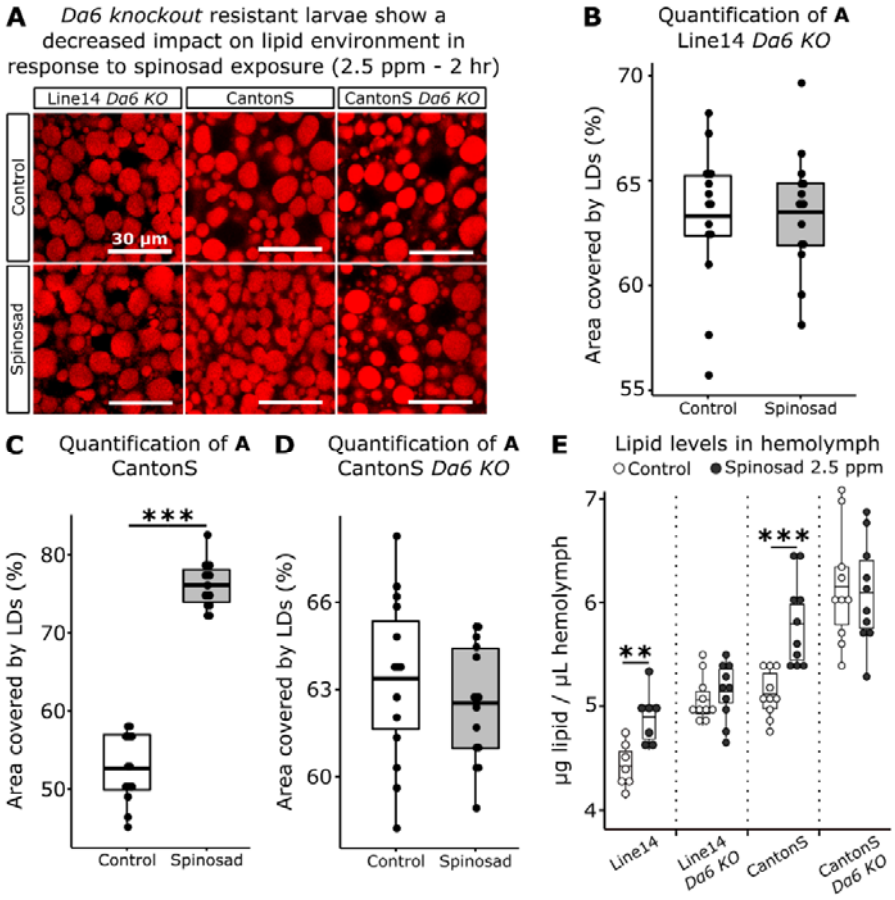

Figure 5. *Da6 knockout* (*KO*) resistant larvae show a decreased impact on lipid environment in response to spinosad exposures. A, Larvae exposed to 2.5 ppm of spinosad for 2 hr. Nile red staining. Images obtained in Leica SP5 Laser Scanning Confocal Microscope, 400x magnification (n = 3 larvae/ treatment; 5 image sections/larva). **B,** Percentage of area occupied by LD in fat body of Line 14 *Da6 KO* larvae. **C,** Percentage of area occupied by LD in fat body of Canton S larvae. **D,** Percentage of area occupied by LD in fat body of Canton S *Da6 KO* larvae. **E,** Amount of lipids in hemolymph (µg/µL) of Line 14 *Da6 KO*, Canton S and Canton S *Da6 KO* larvae exposed to 2.5 ppm spinosad for 2 hr. Measured using the colorimetric vanillin assay (n = 10 replicates/treatment/time-point; 30 larvae/replicate). t-test; ***P < 0.001.

Spinosad triggers major alterations in the lipidome pointing to impaired membrane function and decreased mitochondrial cardiolipins

To further investigate the impacts on the lipid environment we performed a lipidomic analysis on whole larvae exposed to 2.5 ppm spinosad for 2 hr. Significant changes were observed in the levels of 88 lipids out of the 378 detected by mass spectrometry (**Figure 6A**; **Figure 6 – table supplement 1**). A significant portion of the changes in lipids correspond to a reduction in phosphatidylcholine (PC), phosphatidylethanolamine (PE) and some triacylglycerol (TAG) species. Multivariate analysis (**Figure 6B**) indicates that the overall lipidomic profiles of exposed larvae forms a tight cluster that is distinct from the undosed control. The use of whole larvae for lipidomic analysis reduces the capacity to detect significant shifts in lipid levels that predominantly occur in individual tissues but allows the identification of broader impacts on larval biology. In this context, the observed 65% reduction in the levels of identified cardiolipins (CL) is particularly noteworthy (**Figure 6C**). CL are mostly present in mitochondria and are required for the proper function of the TCA cycle proteins, especially those of Complex 1, the major ROS generator when dysfunctional (Quintana et al., 2010; Ren et al., 2014).

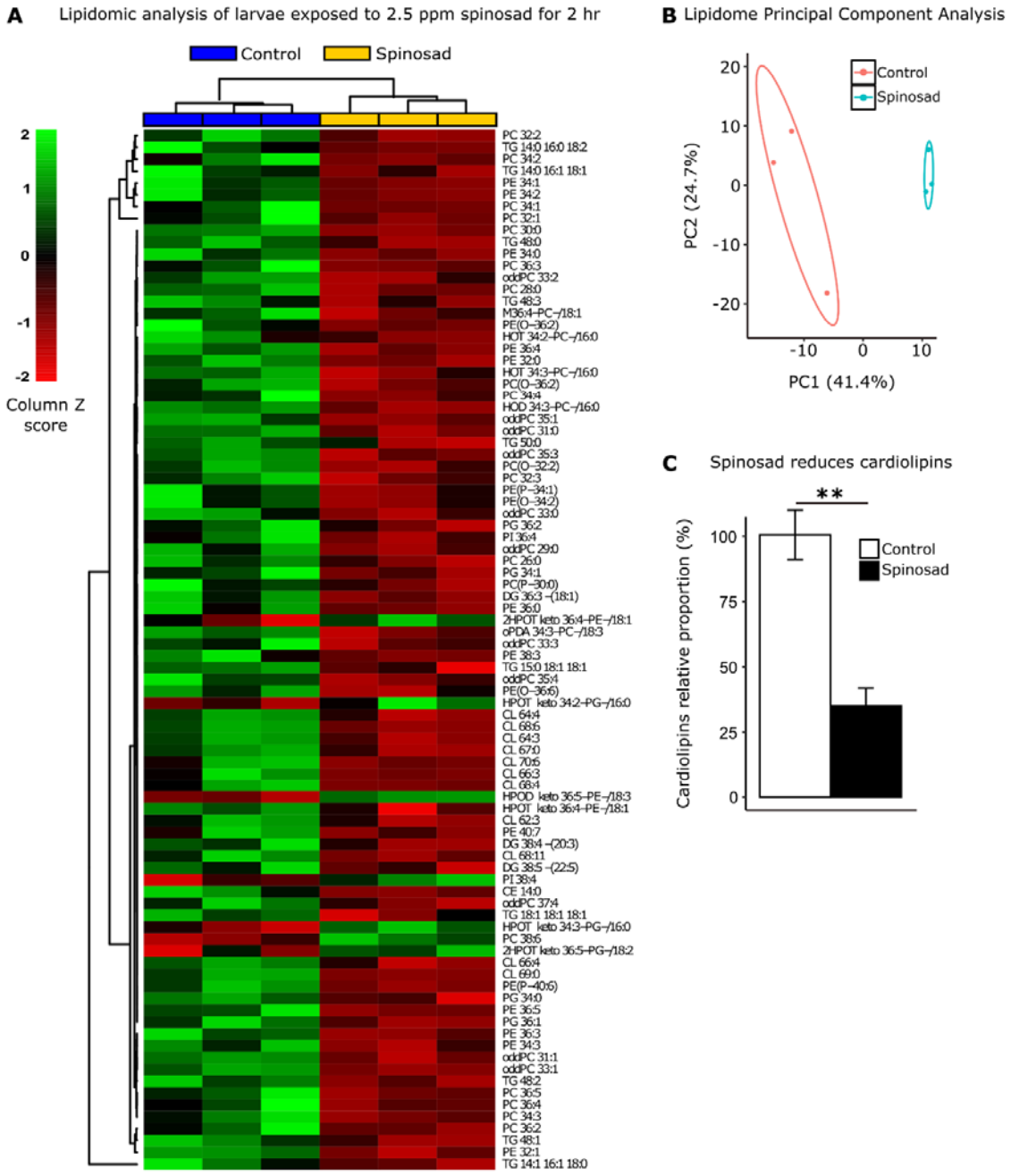

Figure 6. Spinosad disturbs the lipid profile of exposed larvae. Lipidomic profile of larvae exposed to 2.5 ppm spinosad for 2 hr (n = 10 larvae/replicate; 3 replicates/treatment). **A,** 88 lipid species out of the 378 identified were significantly affected by insecticide treatment (One-way ANOVA, Turkey's HSD, $P < 0.05$). The column Z score is calculated subtracting from each value within a row the mean of the row and then dividing the resulting values by the standard deviation of the row. The features are color coded by row with red indicating low intensity and green indicating high intensity. **B,** Principal Component Analysis of 378 lipid species. Each dot represents the lipidome data sum of each sample. First component explains 41.4% of variance and second component explains 24.7% of variance. **C,** Relative proportion of cardiolipins in exposed animals versus control. Error bars in **C** represent mean ± s.e.m. t-test; $^{**}P < 0.01$.

Chronic low exposure to spinosad causes neurodegeneration and progressive loss of vision

Next, we investigated the effects of chronic exposure to spinosad in adults. A dose of 0.2 ppm spinosad kills 50% of adult female flies within 25 days (**Figure 7A**). Two different behavioural assays were initially assessed: bang sensitivity and climbing. Exposure to 0.2 ppm spinosad for 10 and 20 days increased the bang sensitivity phenotype that has been associated with perturbations in synaptic transmission (Saras and Tanouye, 2016) that can arise from various defects including defective channel localization, neuronal wiring and mitochondrial metabolism (Fergestad et al., 2006) (**Figure 7B**). This assay measures the time it takes for flies to recover to a standing position following mechanical shock induced by vortexing the flies. Exposed flies also performed poorly in climbing assays, a phenotype which is often linked to neurodegeneration (McGurk et al., 2015). Indeed, 16%, 73% and 84% of flies failed to climb after 1, 10 and 20 days of exposure, respectively (**Figure 7C**). These data suggest that low doses of spinosad induce neurodegenerative phenotypes.

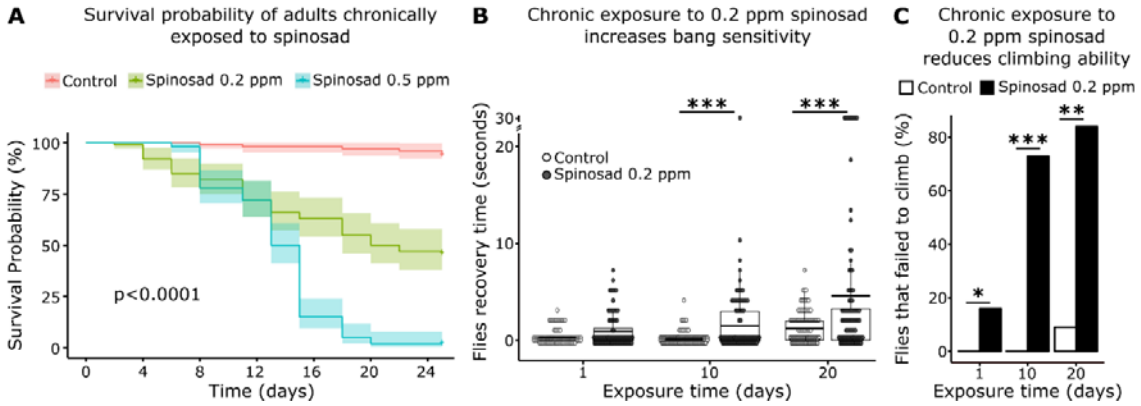

Figure 7. Chronic exposure to spinosad affects behavior. A, Determination of a chronic exposure dose that kills 50% of adults within 25 days. Females adults (2-5 days old) were exposed to different concentrations of spinosad for 25 days (n = 25 flies/ replicate; 4 replicates/ treatment). The dose of 0.2 ppm was selected for assessing the impacts of adult chronic exposures. Shaded areas represent 95% confidence interval (Kaplan-Meier method and the Log-rank Mantel-Cox test). **B,** Chronic exposure to 0.2 ppm spinosad increases bang sensitivity. Bang sensitivity assay of adults after 1, 10 and 20 days of exposure. Groups of 5 flies were vortexed in a clear vial for 10 seconds at maximum speed and the recovery time (time regain normal standing posture) for each fly was recorded (n = 100 flies/time point/ treatment). **C,** Chronic exposure to 0.2 ppm spinosad reduces climbing ability. Percentage of adult flies that failed to climb after 1, 10 and 20 days of exposure (n = 100 flies/ time point/ treatment). **B** and **C**, Wilcoxon test; **P < 0.01; ***P < 0.001.

The retina of adult female flies chronically exposed to 0.2 ppm spinosad were examined for evidence of neurodegeneration, such as the accumulation of LD in glial cells based on Nile Red staining (Liu et al., 2015). Nile Red positive accumulations, likely to represent small LD, were observed decorating the plasma membrane of photoreceptor cells (**Figure 8A, B**). Even though nAChR *Dα6* is not expressed in the retina, it is widely expressed in the adult brain, including the lamina, tissue adjacent to the retina where the photoreceptors synapse (**Figure 8 – figure supplement 1**). Indeed, several laminar neurons synpase with the photoreceptors. The accumulation of LD in neurons suggest that the postsynaptic cells that express D6 somehow affect lipid production in PR.

To quantify possible impacts on visual function, electroretinograms (ERGs) were performed at regular intervals over the 20 days of exposure (**Figure 8C-E**). ERG recordings measure impulses induced by light. The on-transient is indicative of synaptic transmission between photoreceptor neurons (PR) and postsynaptic cells, whilst the amplitude measures the phototransduction cascade (Wang and Montell, 2007). A large reduction in the on-transient was observed from day 1 of exposure, whereas the amplitude was only significantly impacted after 20 days of exposure. The reduction in the on-transient is evidence of a rapid loss of synaptic transmission in laminar neurons (Wang and Montell, 2007) and hence impaired vision after just one day of exposure.

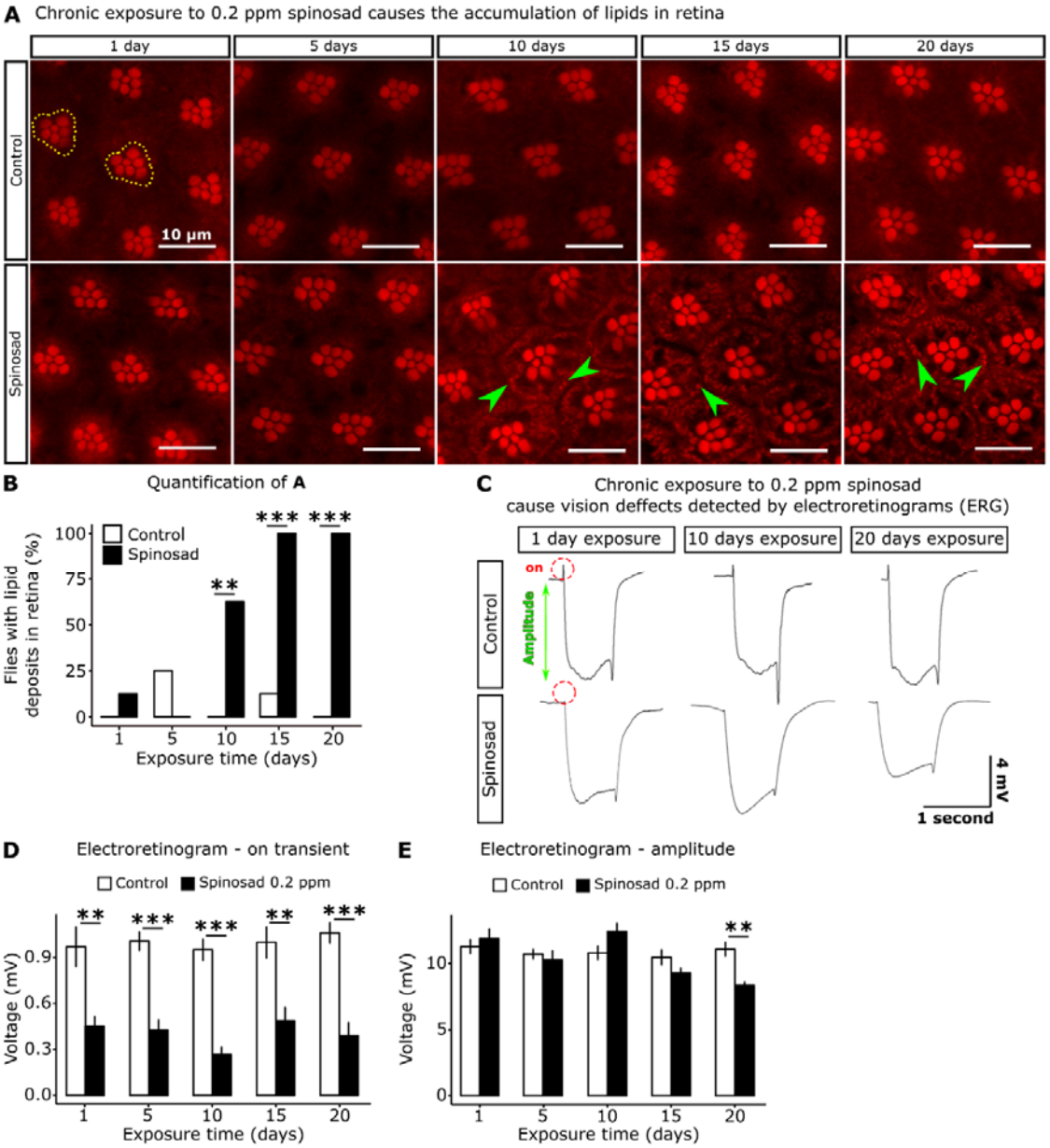

Figure 8. Chronic exposure to spinosad causes loss of vision. A, Clusters of rhabdomeres in the retina. In day 1 – control, two clusters of rhabdomeres are delimited with yellow dotted-lines. A diffuse lipid accumulation is observed from day 10 onwards. Nile red staining. 600 x magnification. **B,** Percentage of animals that shows lipid deposits in the retina (n = 8 flies/treatment/time point). **C,** Electroretinograms (ERGs) of animals exposed to 0.2 ppm spinosad for 1, 10 and 20 days. Red dotted circles indicate the on-transient signal and green arrow indicates the amplitude, (n = 8 to 10 adult flies/time point/treatment). **D,** On-transient signal of ERGs after days 1, 5, 10, 15 and 20 of exposure to 0.2 ppm spinosad. **E,** Amplitude of ERGs after days 1, 5, 10, 15 and 20 of exposure to 0.2 ppm spinosad. Microscopy images obtained in Leica SP5 Laser Scanning Confocal Microscope. t-test; **P < 0.01; ***P < 0.001.

To investigate the ultrastructure of the PR synapses we used Transmission Electron Microscopy. Severe morphological alterations were detected in transverse sections of the lamina of flies exposed for 20 days (**Figure 9A-F**). Vacuoles of photoreceptor terminals or postsynaptic terminals of synapsing neurons were observed in the lamina cartridges (**Figure 9B**). On average 70% of images showed the presence of vacuoles in lamina cartridges (**Figure 9E**). Large intracellular compartments were also observed in the dendrites of the postsynaptic neurons in the lamina (**Figure 9B-D**). These

386 do not correspond to normal structures found in healthy lamina (**Figure 9A**). The lamina of exposed
387 flies also showed a mean 34% increase in the number of mitochondria (**Figure 9F**), many of which
388 appear defective (**Figure 9B**). In examining the visual system of a *Dα6 KO* mutants reared without
389 spinosad, mild impacts were identified in ERG amplitude but a very significant reduction in on-
390 transient was observed, consistent with a requirement for *Dα6* in postsynaptic cells of the
391 photoreceptors. No morphological alterations were detected in the lamina by TEM (**Figure 9 – figure**
392 **supplement 1**).

393 Lastly, Hematoxylin & Eosin stain (H&E) of adult flies painted a picture of the neurodegeneration
394 caused outside the visual system by chronic low dose exposure to spinosad. 20 days of exposure
395 caused numerous vacuoles in the central brain (**Figure 9G, H**). On average, 17% of the total central
396 brain area was consumed by vacuoles in exposed flies.

397

398

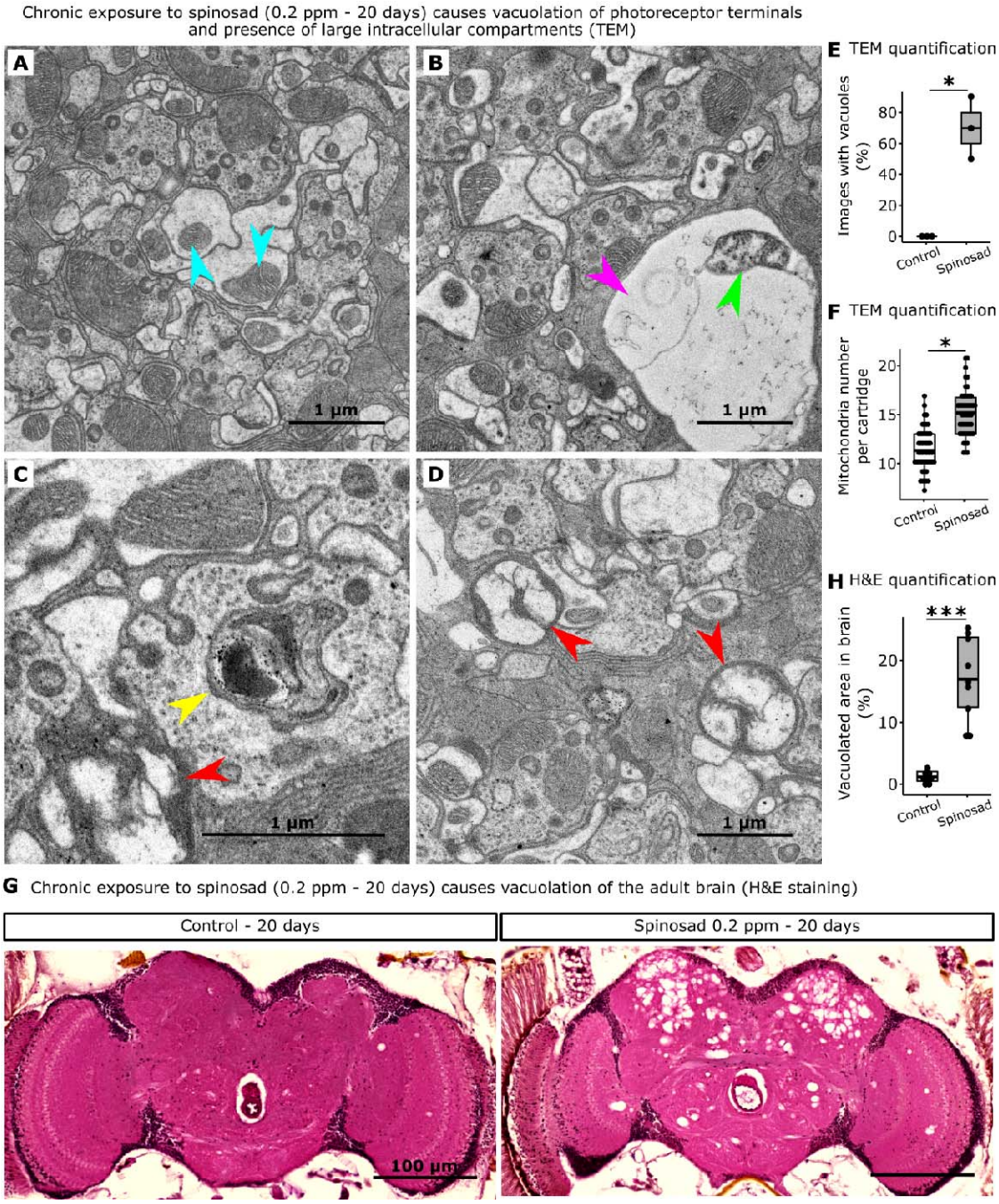

Figure 9. Chronic exposure to spinosad causes neurodegeneration. A, Transmission electron microscopy (TEM) of the lamina of a control animal showing a regular cartridge, blue arrowheads indicate normal mitochondria. **B-D,** TEM of lamina of flies exposed to 0.2 ppm spinosad for 20 days. **B,** Pink arrowhead indicates vacuole and green arrowhead indicates a defective mitochondrion. **C,** Yellow arrowhead indicates an enlarged digestive vacuole inside a photoreceptor terminal. **D,** Red arrowheads indicate the presence of large unidentified intracellular compartments. **E,** Percentage of images showing vacuoles in lamina cartridges (10 images/fly; 3 flies/ treatment). **F,** Number of mitochondria per cartridge (n = 3 flies/group; 16 cartridges/fly). **G,** Flies exposed to 0.2 ppm spinosad for 20 days show vacuolation of the central brain. Brain frontal sections stained with hematoxylin and eosin (H&E). **H,** Quantification of neurodegeneration in terms of percentage of brain area vacuolated (n = 3 flies/treatment). t-test; *P < 0.05; ***P < 0.001.

Discussion

Spinosad antagonizes neuronal activity

In this study we provide evidence of the mechanism and consequences of exposure to low doses of spinosad. This organic insecticide leads to a lysosomal dysfunction associated with a mitochondrial dysfunction, elevated levels of ROS, lipid mobilization defects and neurodegeneration. Spinosad has been characterized as an allosteric modulator of the activity of its primary target, the nAChR – Dα6 subunit, causing fast neuron over-excitation (Salgado, 1998). Here, the capacity of spinosad to interact with its target nAChRs to stimulate the flux of Ca^{2+} into neurons was quantified. The results obtained with the GCaMP assay showed that spinosad caused no detectable increase or decrease in Ca^{2+} flux into *Dα6* expressing neurons, but it reduced the cholinergic response (**Figure 1**). Given that spinosad binds to the C terminal region of the protein (Crouse et al., 2018; Puinean et al., 2013; Somers et al., 2015), these findings are consistent with a non-competitive antagonist mode of action for spinosad on nAChRs. That *Dα6* loss of function mutants are viable (Perry et al., 2007) creates a conundrum that can be resolved if a significant component of spinosad's toxicity is due to molecular events that play out elsewhere in the cell. Blocked neuronal receptors can be recycled from the plasma membrane through endocytosis (Saheki and De Camilli, 2012). Our data indicate that spinosad exposure leads to the removal of Dα6 nAChRs from neuronal membranes (Nguyen et al., 2021) and localization to enlarged lysosomes, resulting in lysosomal expansion (**Figure 2C**) and lysosomal dysfunction.

Spinosad causes lysosomal storage diseases - like phenotype

The following observations suggest that spinosad induces lysosomal dysfunction. LysoTracker staining reveals a very significant accumulation of enlarged lysosomes in the brain in response to spinosad, but not in the presence of imidacloprid, another insecticide which also binds to nAChRs (**Figure 2 – figure supplement 1**). Importantly, *Dα6 knockout* flies show no accumulation of LysoTracker staining, clearly showing that the lysosomal lesions rely on the presence of Dα6 and spinosad (**Figure 2 – figure supplement 1**). Whether spinosad molecules are ferried to lysosomes along with Dα6 subunits and accumulate into these organelles remains to be clarified. However, the increased severity in the lysosomal phenotype after exposure ceases (**Figure 2A, B**) is consistent with the poisoning of these organelles. Lysosomes become enlarged as they accumulate undigested material, which can lead to recycling problems for neurons (Darios and Stevanin, 2020). If spinosad remains bound to the receptor and is ferried into the lysosomes it may contribute to a lysosomal dysfunction akin to Lysosomal Storage Disease (LSD) (Darios and Stevanin, 2020). To date there is little published evidence of spinosad metabolites in insects. Spinosad is a complex polyketide macrolactone that may not be hydrolysed by lysosome acidic enzymes and could accumulate in the lumen of these organelles.

Our hypothesis for the mode of action of spinosad is illustrated in **Figure 10**. Spinosad exposure shows a delayed effect on larval movement when compared to imidacloprid (Denecke et al., 2015; Martelli et al., 2020). We attribute this to the time taken for a threshold level of lysosomal damage to accumulate. Imidacloprid is readily metabolized and the metabolites are excreted (Fusetto et al., 2017), leaving little lingering damage. In contrast, following a 2hr exposure to 2.5ppm spinosad, 3rd instar larvae show a developmental arrest and die after several days (**Figure 1**). The LSD-like dysfunction is also likely the underlying cause for the severe vacuolation of adult central brain under spinosad chronic exposure. Recycling defects in neuronal cells caused by LSD impair cell function, ultimately triggering neurodegeneration (Darios and Stevanin, 2020). Nguyen et al. (2021) recently showed that flies treated with a proteasome inhibitor drug, bortezomib, present with a reduced loss of Dα6 from neuronal membranes when exposed to spinosad. That suggests that the proteasome degradation pathway could also be involved in recycling spinosad-blocked Dα6 subunits. Receptors marked for proteasome degradation can end up in lysosomes as these pathways engage in crosstalk (Korolchuk et al., 2010).

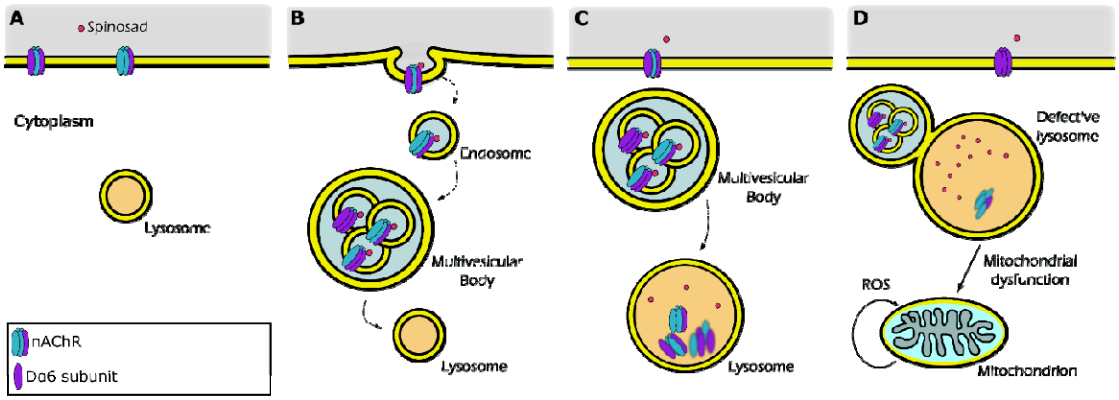

Figure 10. Proposed mechanism for internalization of spinosad after binding to the Dα6 nAChR target. A, Spinosad binds to Dα6 subunit of nAChRs in the neuronal cell membranes. **B,** The binding of spinosad leads to Dα6 nAChR blockage, endocytosis and trafficking to lysosome**. C,** Spinosad accumulates in lysosomes, while receptors and other membrane components are digested. **D,** Enlarged lysosomes due to accumulation of undigested material do not function properly leading to cellular defects which may include mitochondrial dysfunction, increased mitochondrial ROS production and eventually cell vacuolation and neurodegeneration.

Spinosad triggers oxidative stress

Extensive evidence connects lysosomal disorders with mitochondrial dysfunction (Plotegher and Duchen, 2017; Stepien et al., 2020; Yambire et al., 2018). Mitochondrial dysfunction is widespread in LSD and is involved in its pathophysiology. Although mitochondrial dysfunction in LSD seems to have a multifactorial origin, the exact mechanisms remain unclear. Lysosomal disorders may lead to cytoplasmic accumulation of toxic macromolecules, impaired degradation of damaged mitochondria and dysregulation of intracellular Ca^{2+} homeostasis, resulting in increased ROS generation and reduced ATP levels (Plotegher and Duchen, 2017). The severe lysosomal dysfunction observed here is the most likely cause for the mitochondrial defects and increased ROS generation triggered by spinosad exposure.

The evidence for oxidative stress produced during spinosad exposure comes from the accumulation of superoxide, increased mitochondrial turnover, reduced activity of the ROS sensitive enzyme m-aconitase and reduced ATP levels (**Figure 3**), accumulation of LD in fat bodies (**Figure 4**), and severe reduction of cardiolipin levels that typically associated with defects in the electron transport chain and increased ROS production (Quintana et al., 2010) (**Figure 6**). Increasing levels of ROS in the larval brain using RNAi has been shown to disturb mitochondrial function triggering changes in lipid stores in metabolic tissues (Martelli et al., 2020). Oxidative stress promotes redistribution of membrane lipids into LD, reducing their susceptibility to lipid peroxidation (Bailey et al., 2015). Here, increases in lipid stores were observed in the fat body, with a reduction in the numbers of large LD and accumulation of small LD, a reduction in LD in the Malpighian tubules and midgut and changes in lipid levels in the hemolymph (Figure (**Figure 4**). Our lipidome analysis revealed reduction of PE and PC levels (**Figure 6**), consistent with impaired membrane fluidity and altered LD dynamics (Dawaliby et al., 2016; Guan et al., 2013; Krahmer et al., 2011).

The use of the antioxidant NACA reduces the accumulation of LD in the fat body linking this phenotype to oxidative stress (**Figure 4**). NACA also diminished spinosad toxicity by reducing the impact on larval movement and survival (**Figure 4**). *Dα6 knockout* mutants exposed to spinosad show no accumulation of LD in the fat body or change of lipid levels in hemolymph indicating that these phenotypes are due to the spinosad:Dα6 interaction (**Figure 5**). Exposed to 7.7 ppb (parts per billion) for 24 hr was shown to cause the vacuolation of epithelial cells of the midgut and Malpighian tubules of honeybees (*Apis mellifera*) (Lopes et al., 2018). It is not clear whether this is due to the spinosad:Dα6 interaction precipitating elevated levels of ROS.

A striking similarity between impacts caused in metabolic tissues by spinosad and imidacloprid (Martelli et al., 2020) is observed, although the impacts induced by spinosad are more severe. In the

case of imidacloprid, these perturbations were shown to be caused by an oxidative stress signal initiated by an increase Ca^{2+} influx into neurons caused by the insecticide binding to its nAChR targets (Martelli et al., 2020). It was proposed that peroxidised lipids generated in the brain and carried in hemolymph precipitate oxidative damage to other tissues (Ioannou et al., 2019; Valko et al., 2007). Concomitantly, *Da6* has been associated with the response to oxidative stress. *Da6* mutants are more susceptible to oxidative damage (Weber et al., 2012). Studies on genes of the mammalian α7 family, which includes *Drosophila Dα6* gene, have been shown to play a role in neuroprotection by inducing the antioxidant system through Jak2/STAT3 pathway (Egea et al., 2015). Therefore, an absence of Dα6 subunits from neuronal membranes under conditions of spinosad exposure may increase susceptibility to oxidative damage.

Lysosomal dysfunction provides a parsimonious explanation as the cause for the mitochondrial impairment and ROS generated by spinosad exposure (Deus et al., 2020; Plotegher and Duchen, 2017; Stepien et al., 2020; Yambire et al., 2018) (**Figure 10**). But the accumulation of superoxide was observed earlier (1 hr) than the lysosomal defects (2 hr), although levels of Dα6 protein were shown to have decreased significantly after 30 min (**Figure 2 – figure supplement 2**). This could be explained by different capacities of DHE and LysoTracker to detect thresholds of damage that have a significant biological impact. However, it also leaves open the possibility that the generation of ROS is due to another mechanism that probably relates to the severe lowering of cardiolipins in mitochondrial membranes.

Spinosad causes neurodegeneration and affects behavior in adults

Both LSD (Darios and Stevanin, 2020) and oxidative stress (Liu et al., 2017; Martelli et al., 2020) can cause neurodegeneration. The evidence for spinosad-induced neurodegeneration comes from the reduced climbing ability caused by chronic low dose exposures (McGurk et al., 2015; **Figure 7**), blindness (**Figure 8**), vacuolation of the lamina cartridges and severe vacuolation of adult CNS (**Figure 9**). Electroretinograms reveal that both *Dα6 knockout* mutants non-exposed and wild type flies chronically exposed to 0.2 ppm spinosad have reduced on-transients and amplitudes in response to light flashes (**Figure 8; Figure 9 – figure supplement 1**). *Dα6 knockout* mutants, however, show no vacuolation of lamina (**Figure 9 – figure supplement 1**). Given that *Dα6 knockout* mutants are viable, highly resistant to spinosad and show no conspicuous behavioral defects, it becomes clear that the majority of the impacts caused by spinosad are not initiated by the absence of Dα6 from neuronal membranes. The astonishing level of neurodegeneration observed in the central brain (**Figure 9G, H**) seems to be largely contained to the functional regions of the optic tubercle, mushroom body and superior lateral and medial protocerebrum. These regions are important centres for vision and memory, and learning and cognition in flies (Schürmann, 2016). Neurodegeneration in these regions indicate that a wide range of behaviours would be critically compromised in exposed flies.

Da6 nAChRs are not known to be expressed in photoreceptor cells or glial cells, but their expression in lamina (**Figure 8 – figure supplement 1**) supports their presence in post-synaptic cells. The accumulation of LD in PR after spinosad exposure (**Figure 8A**) suggests the existence of cell non-autonomous mechanisms initiated by spinosad in post-synaptic cells. Liu et al. (2017) showed that ROS induce the formation of lipids in neurons that are transported to glia, where they form LD. Here, a ROS signal generated by spinosad exposure in post-synaptic cells might be carried to PR, affecting lipid metabolism, and triggering LD accumulation. This hypothesis needs further investigation.

Rational control of insecticide usage

In the public domain, organic insecticides are often assumed to be safer than synthetic ones for the environment and non-target insect species. The synthetic insecticide, imidacloprid, has faced intense scrutiny and bans because of its impact on the behavior of bees and the potential for this to contribute to the colony collapse phenomenon (Wu-Smart and Spivak, 2016). No other insecticide has been so comprehensively investigated, so it is not yet clear whether other chemicals pose similar risks. This study has revealed disturbing impacts of low doses of an organic insecticide, spinosad. Using the same methods deployed here, imidacloprid had a lower impact in *Drosophila* than spinosad (Martelli et al., 2020). At the same low acute dose (2.5 ppm for 2 hr), imidacloprid has no impact on larval survival, while spinosad is lethal. 4 ppm imidacloprid causes blindness and neurodegeneration, but no brain vacuolation under conditions of chronic exposure with 56% of flies dying in 25 days. 0.2ppm

spinosad causes blindness and widespread brain vacuolation with 54% of flies dying in 25 days. That the nAChR Dα6 subunit has been shown to be a highly conserved spinosad target across a wide range of insects (Perry et al., 2015) suggests that low doses of this insecticide may have similar impacts in other species. The susceptibility of different species to insecticides varies, so the doses required may differ between them. The protocols used here will be useful in assessing the risk that spinosad poses to beneficial insects. Given the extent to which spinosad affects mitochondrial function, lipid metabolism and the brain, this insecticide may compromise the capacity of insects to survive in natural populations exposed to a variety of stresses including some of those that are being linked to insect population declines (Cardoso et al., 2020; Sánchez-Bayo and Wyckhuys, 2019).

Two clocks are ticking. The global human population is increasing and the amount of arable land available for food production is decreasing. Thus, the amount of food produced per hectare needs to increase. Our capacity to produce enough food has been underpinned by the use of insecticides. Approximately 600,000 tonnes of insecticides are used annually around the world (Aizen et al., 2009; Klein et al., 2007), but sublethal concentrations found in contaminated environments can affect behaviour, fitness and development of target and non-target insects (Müller, 2018). Despite their distinct modes of action, spinosad and imidacloprid produce a similar spectrum of damage (Martelli et al., 2020). This similarity arises because both insecticides trigger oxidative stress in the brain, albeit via different mechanisms. Several other insecticide classes such as organochlorines, organophosphates, carbamates and pyrethroids have all been shown to promote oxidative stress (Balieira et al., 2018; Karami-Mohajeri and Abdollahi, 2011; Lukaszewicz-Hussain, 2010; Terhzaz et al., 2015; Wang et al., 2016). Many insect populations are exposed to a continuously changing cocktail of insecticides (Kerr, 2017; Tosi et al., 2018), most of which are capable of producing ROS. The cumulative impact of these different insecticides could be significant. Our research clarifies the mode of action of spinosad, highlighting the perturbations and damage that occur downstream of the insecticide:receptor interaction. Other chemicals should not be assumed to be environmentally safe until their low dose biological impacts have been examined in similar detail.

Material and Methods

Fly strains and rearing

Armenia[14] (Line 14), an isofemale line derived from Armenia[60] (Drosophila Genomics Resource Center #103394) (Perry et al., 2008), was used as the susceptible wild type line for all assays except the following. Expression of nAChR-*Dα6* gene in adult brains: *Dα6* T2A Gal4 (BDSC #76137) was crossed with UAS-GFP.nls (BDSC #4775). Insecticide impact on mitochondrial turnover: the MitoTimer line (Gottlieb and Stotland, 2015) was used. GCaMP experiment: UAS-tdTomato-P2A-GCaMP5G (III) (Daniels et al., 2014; Wong et al., 2014) was crossed with *Dα6* T2A Gal4 (BDSC #76137). Two mutants for the nAChR-*Dα6* gene, which confers resistance to spinosad (Perry et al 2015) and their background control lines were used to investigate the insecticide mode of action. The first of these is Line 14 *Dα6 KO* strain, a mutant recovered following EMS mutagenesis in the Line 14 genetic background, with no detectable *Dα6* expression (Perry et al., 2015). The second mutant is a CRISPR knockout of *Dα6* generated in the CantonS genetic background. For experiments aiming to investigate the trafficking of *Dα6* nAChR in brains, UAS *Dα6* CFP tagged strain built in Line 14 *Dα6 KO* background (obtained by CRISPR) was crossed to a Gal4-L driver in Line 14 *Dα6 KO* background strain. For experiments involving larvae, flies were reared on standard food media sprinkled with dried yeast and maintained at 25°C. For experiments involving adults, flies were reared in molasses food and maintained at 25°C. In all experiments involving adult flies only females were used to maintain consistency.

Insecticide dilution and exposure

The pure version of spinosad (Sigma Aldrich®) was used in all assays. The chemical was diluted to create 1000 ppm stocks solution, using dimethyl sulfoxide (DMSO), and was kept on freezer (-20°C). Before exposures, 5x stocks were generated for the dose being used by diluting the 1000 ppm stock in 5% Analytical Reagent Sucrose (Chem Supply) solution (or equivalent dose of DMSO for controls).

627 Antioxidant treatment

628 The antioxidant, N-acetylcysteine amide (NACA) was used as previously described (Martelli et al.,
629 2020). Briefly, larvae were treated with 300 µg/mL of NACA in 5% Analytical Reagent Sucrose (Chem
630 Supply) solution for 5 hr prior to exposure to spinosad exposures.

631 Fly medias used

Standard Food (1L)		***Apple Juice Plates (1L)***		***Molasses Food (1L)***	
H_2O	987 mL	*H_2O*	720 mL	*H_2O*	800 mL
Potassium Tartrate	8.0 g	*Agar*	20 g	*Molasses*	160 mL
Calcium Chloride	0.5 g	*Apple Juice*	200 mL	*Maize meal*	60 g
Agar	5.0 g	*Brewer's Yeast*	7.0 g	*Dried active yeast*	15 g
yeast	12 g	*Glucose*	52 g	*Agar*	6.0 g
Glucose	53 g	*Sucrose*	26 g	*Acid mix*	7.5 mL
Sucrose	27 g	*Tegosept*	6.0 mL	*Tegosept*	5.0 mL
Semolina	67 g				
Acid Mix	12 mL				
Tegosept	15 mL				

632

633 Larvae movement assay

634 Larvae movement in response to insecticide exposure was quantified by Wiggle Index Assay, as
635 described by Denecke et al. (2015). 25 third instar larvae were used for a single biological replicate
636 and four replicates were tested for each exposure condition. Undosed larvae in NUNC cell plates
637 (Thermo-Scientific) in 5% Analytical Reagent Sucrose (Chem Supply) solution were filmed for 30
638 seconds and then 30 min, 1 hr, 1 hr and 30 min and 2 hr after spinosad exposure. The motility at each
639 time-point is expressed in terms of Relative Movement Ratio (RMR), normalized to motility prior to
640 spinosad addition.

641 Larvae viability and adult survival tests

642 For all tests 5 replicates of 20 individuals (100 individuals) per condition were used. In assessing third
643 instar larval viability and metamorphosis following insecticide exposure, individuals were rinsed three
644 times with 5% w/v sucrose (Chem Supply) and placed in vials on insecticide-free food medium.
645 Survival probability of larvae exposed to 2.5 ppm spinosad for 2 hr was analysed using Kaplan-Meier
646 method and the Log-rank Mantel-Cox test. Correct percentage survival of larvae exposed to 0.5 ppm
647 spinosad for 2 hr, or 0.1 ppm spinosad for 4 hr was analysed using Abbots' correction. To examine
648 the survival of adult flies chronically exposed to 0.2 ppm spinosad, 5 replicates of 20 females (3-5
649 days old) were exposed for 25 days. The same number of flies was used for the control group.
650 Statistical analysis was based on the Kaplan-Meier method and data were compared by the Log-rank
651 Mantel-Cox test.

652 GCaMP assay

653 Cytosolic [Ca2+] in *Drosophila* primary neurons was measured as previously described (Martelli et al.,
654 2020). Briefly, four brains from third instar larvae were dissected to generate ideal number of cells for
655 3 plates. Cells were allowed to develop in culture plates (35 mm glass-bottom dishes with 10 mm
656 bottom well (Cellvis), coated with concanavalin A (Sigma)) with Schneider's media for 4 days with the
657 media refreshed daily. Recording was done using a Nikon A1 confocal microscope, 40x air objective,
658 sequential 488nm and 561nm excitation. Measurements were taken at 3 second intervals. Cytosolic
659 Ca^{2+} levels were reported as GCaMP5G signal intensity divided by tdTomato signal intensity. Signal
660 was recorded for 60 sec before the addition of 2.5 ppm or 25 ppm spinosad to the bath solution. 5 min
661 after that, both insecticide and control groups were stimulated by the cholinergic agonist carbachol
662 (100 µM) added to the bath solution, and finally the SERCA inhibitor thapsigargin (5 µM) was added

after a further 1 min. At least 50 neuronal cells were evaluated per treatment. The data were analysed using a Student's t-test.

Evaluation of mitochondrial turnover

Mitochondrial turnover was assessed as previously described (Martelli et al., 2020). Larvae of the MitoTimer line were exposed to 2.5 ppm spinosad for 2 hr. Control larvae were exposed to 2.5ppm DMSO. Midguts and brains were dissected in PBS and fixed in 4% PFA (Electron Microscopy Science) and mounted in Vectashield (Vector Laboratories). 20 anterior midguts and 20 pairs of optical lobes were analysed for each condition. Confocal microscopy images were obtained in Leica SP5 Laser Scanning Confocal Microscope at 200x magnification for both green (excitation/emission 488/518 nm) and red (excitation/emission 543/572 nm) signals. Three independent measurements along the z stack were analysed for each sample. Fluorescence intensity was quantified on ImageJ software and data were analysed using a Student's t-test.

Systemic mitochondrial aconitase activity

Relative mitochondrial aconitase activity was quantified using the colorimetric Aconitase Activity Assay Kit from Sigma (#MAK051), following manufacturer's instructions as previously described (Martelli et al., 2020). A total of six biological replicates (25 whole larvae per replicate) were exposed to 2.5 ppm spinosad for 2 hr, whilst six control replicates (25 whole larvae per replicate) were exposed to DMSO for 2 hr. Absorbance was measured at 450 nm in a FLUOstar OPTIMA (BMG Labtech) microplate reader using the software OPTIMA and normalized to sample weight. The data were analysed using a Student's t-test.

Systemic ATP levels

Relative ATP levels were quantified fluorometrically using an ATP assay kit (Abcam, #83355), following manufacturer instructions as previously described (Martelli et al., 2020). A total of six biological replicates (20 larvae per replicate) were exposed to 2.5 ppm spinosad for 2 hr, whilst six control replicates (20 larvae per replicate) were exposed to DMSO for 2 hr. Fluorescence was measured at excitation/emission = 535/587 nm in FLUOstar OPTIMA (BMG Labtech) microplate reader using the software OPTIMA and normalized to sample weight. The data were analysed using a Student's t-test.

Measurement of superoxide (O_2^-) levels

Levels of superoxide were assessed dihydroethidium staining (DHE – Sigma-Aldrich), as described in (Owusu-Ansah et al. 2008). Briefly, larvae were dissected in Schneider's media (GIBCO) and incubated with DHE at room temperature on an orbital shaker for 7 minutes in dark. Tissues were fixed in 8% PFA (Electron Microscopy Science) for 5 minutes at room temperature on an orbital shaker in dark. Tissues were then rinsed with PBS (Ambion) and mounted in Vectashield (Vector Laboratories). Confocal microscopy images were obtained in a Leica SP5 Laser Scanning Confocal Microscope at 200x magnification (excitation/emission 518/605 nm). Third instar larvae were exposed to 2.5 ppm spinosad for 1 or 2 hr. Controls were exposed to equivalent doses of DMSO. A total of 15 brains and 15 midguts were assessed for each condition. Three independent measurements along the z stack were analysed for each sample. Fluorescence intensity was quantified on ImageJ software and data were analysed using a Student's t-test.

Evaluation of lipid environment of metabolic tissues in larvae

Fat bodies, midguts and Malpighian tubules were dissected in PBS (Ambion) and subjected to lipid staining with Nile Red N3013 Technical grade (Sigma-Aldrich) as previously described (Martelli et al., 2020). Three biological replicates were performed for each exposure condition, each replicate consisting of a single tissue from a single larva. Tissues were fixed in 4% PFA (Electron Microscopy Science) and stained with 0.5 µg/mL Nile Red/PBS for 20 minutes in dark. Slides were mounted in Vectashield (Vector Laboratories) and analysed using a Leica SP5 Laser Scanning Confocal Microscope at 400x magnification. Red emission was observed with 540 ± 12.5 nm excitation and 590 LP nm emission filters. Images were analysed using ImageJ software. For fat bodies, the number, size and percentage of area occupied by lipid droplets was measure in 5 different random sections of

2500 µm^2 per sample (three samples per group). For Malpighian tubules number of lipid droplets was measure in five different random sections of 900 µm^2 per sample (three samples per group). For midgut samples, lipid droplets were not quantified, rather zones containing lipid droplets were identified by microscopy. The data were analysed using Student's t-test.

Lipid quantification in larvae hemolymph

Extracted hemolymph lipids were measured using the sulfo-phospho-vanillin method (Cheng et al. 2011) as previously described (Martelli et al., 2020). 30 third instar larvae were used for a single biological replicate and 7 replicate samples were prepared for each exposure condition. Absorbance was measured at 540 nm in a CLARIOstar® (BMG LABTECH) microplate reader using MARS Data Analysis Software (version 3.10 R3). Cholesterol (Sigma-Aldrich) was used for the preparation of standard curves. The data were analysed using a Student's t-test.

Lipid Extraction and Analysis Using Liquid Chromatography-Mass Spectrometry.

Lipidomic analyses of whole larvae exposed for 2 h to 2.5 ppm spinosad were performed in biological triplicate and analyzed by electrospray ionization-mass spectrometry (ESI-MS) using an Agilent Triple Quad 6410 as previously described (Martelli et al., 2020). Briefly, samples were transferred to CryoMill tubes treated with 0.001% BHT (butylated hydroxytoluene) and frozen in liquid nitrogen. Samples were subsequently homogenized using a CryoMill (Bertin Technologies) at −10 °C. Then 400 µL of chloroform was added to each tube and samples were incubated for 15 min at room temperature in a shaker at 1,200 rpm. Samples were then centrifuged for 15 min, at 13,000 rpm at room temperature; the supernatants were removed and transferred to new 1.5-mL microtubes. For a second wash, 100 µL of methanol (0.001% BHT and 0.01 g/mL 13C5 valine) and 200 µL of chloroform were added to CryoMill tubes, followed by vortexing and centrifugation as before. Supernatants were transferred to the previous 1.5-mL microtubes. A total of 300 µL of 0.1 M HCl was added to pooled supernatants and microtubes were then vortexed and centrifuged (15 min, room temperature, 13,000 rpm). Upper phases (lipid phases) were collected and transferred to clean 1.5-mL microtubes, as well as the lower phases (polar phases). All samples were kept at −20 °C until analysis. For liquid chromatography-mass spectrometry (LC-MS) analysis, microtubes were shaken for 30 min at 30 °C, then centrifuged at 100 rpm for 10 min at room temperature after which the supernatants were transferred to LC vials. Extracts were used for lipid analysis. For statistical analysis the concentration of lipid compounds was initially normalized to sample weight. Principal Components Analysis (PCA) was calculated to verify the contribution of each lipid compound in the variance of each treatment. PCA was calculated using the first two principal component axes. To discriminate the impacts of spinosad on the accumulation of specific lipid compounds we performed a One-way ANOVA test with post-hoc Tukey's HSD ($p<0.05$).

Investigating impacts on lysosomes

To investigate spinosad impacts on lysosomes the LysoTracker staining was used on larval brains dissected from 3rd instars. Larvae were exposed to 2.5 ppm spinosad for 1 hr or 2 hr, in the last case brains were assessed immediately after the 2 hr exposure or 6 hr after that. Larvae were dissected in PBS and tissue immediately transferred to PBS solution containing LysoTracker Red DND-99 (1:10,000) (Invitrogen) for 7 minutes. Tissues were then rinsed 3 times in PBS and slides were mounted for immediate microscopy 400x magnification (DsRed filter). A total of 7 brain samples were assessed per group, with 3 random different sections of 900 µm^2 accounted per brain. To investigate the hypothesis of Dα6 nAChRs being endocytosed and digested by lysosomes after exposure to 2.5 ppm spinosad for 2 hr, brains from larvae obtained by crossing UAS *Dα6* CFP tagged in Line 14 *Dα6 KO* strain to Gal4-L driver in Line 14 *Dα6 KO* strain were also subjected to LysoTracker staining. Images were analysed using the software ImageJ and data were analysed using Student's t-test.

Electrophysiology of the retina

Amplitudes and on transients were assessed as previously described (Martelli et al., 2020). Briefly, adult flies were anesthetized and glued to a glass slide. A reference electrode was inserted in the back of the fly head and the recording electrode was placed on the corneal surface of the eye, both electrodes were filled with 100 mM NaCl. Flies were maintained in the darkness for at least 5 min prior to a series of 1 s flashes of white light delivered using a halogen lamp. During screening 8 to 10

765 flies per treatment group were tested. For a given fly, amplitude and on transient measurements were
766 averaged based on the response to the 3 light flashes. Responses were recorded and analysed using
767 AxoScope 8.1. The data were analysed using Student's t-test.

768 Nile red staining of adult retinas

769 For whole mount staining of fly adult retinas, heads were dissected in cold PBS (Ambion) and fixed in
770 37% formaldehyde overnight. Subsequently, the retinas were dissected and rinsed several times with
771 1× PBS and incubated for 15 minutes at 1:1000 dilution of PBS with 1 mg/ml Nile Red (Sigma).
772 Tissues were then rinsed with PBS and immediately mounted with Vectashield (Vector Labs) for
773 same-day imaging. For checking the effects of chronic exposures 8 retinas from 8 adult female flies
774 were analysed per condition (imidacloprid 4 ppm and control) per day (after 1, 5, 10, 15 and 20 days
775 of exposure). Images were obtained with a Leica TCS SP8 (DM600 CS), software LAS X, 600x
776 magnification, and analysed using ImageJ. The data were analysed using Student's t-test.

777 Expression of Dα6 nAChRs in brain

778 The expression patter of nAChR-Dα6 gene in adult brains was assessed in the crossing between Dα6
779 T2A Gal4 (BDSC #76137) and UAS-GFP.nls (BDSC #4775). Adult brains were fixed in 4% PFA
780 (Electron Microscopy Science) in PBS for 20 minutes at room temperature. PFA was removed and
781 tissues were washed 3 times in PBS. Samples were mounted in Vectashield (Vector Laboratories).
782 Images were obtained with a Leica TCS SP8 (DM600 CS), software LAS X, 400x magnification, using
783 GFP channel. Images were analysed using the software ImageJ.

784 Adult brain histology (Hematoxylin & Eosin staining)

785 Adult fly heads were fixed in 8% glutaraldehyde (EM grade) and embedded in paraffin. Sections (10
786 µm) were prepared by a microtome (Leica) and stained with Hematoxylin and Eosin as described
787 (Chouhan et al., 2016). At least three animals were examined for each group (20 days exposure to
788 0.2 ppm spinosad plus control group) in terms of percentage of brain area vacuolated. The data were
789 analysed using Student's t-test.

790 Transmission Electron Microscopy (TEM)

791 Laminas of adult flies chronically exposed to 0.2 ppm spinosad 20 days (controls exposed to
792 equivalent volume of DMSO) were processed for TEM imaging as described (Luo et al., 2017). TEM
793 of laminas of 20-day old CantonS and CantonS *Dα6 KO* mutants aged in the absence of spinosad
794 was also investigated. Samples were processed using a Ted Pella Bio Wave microwave oven with
795 vacuum attachment. Adult fly heads were dissected at 25 °C in 4 % paraformaldehyde, 2 %
796 glutaraldehyde, and 0.1 M sodium cacodylate (pH 7.2). Samples were subsequently fixed at 4 °C for
797 48 hr. 1 % osmium tetroxide was used for secondary fixation with subsequent dehydration in ethanol
798 and propylene oxide. Samples were then embedded in Embed-812 resin (Electron Microscopy
799 Science, Hatfield, PA). 50 nm ultra-thin sections were obtained with a *Leica UC7* microtome and
800 collected on Formvar-coated copper grids (Electron Microscopy Science, Hatfield, PA). Specimens
801 were stained with 1 % uranyl acetate and 2.5 % lead citrate and imaged using a JEOL JEM 1010
802 transmission electron microscope with an AMT XR-16 mid-mount 16 mega-pixel CCD camera. For
803 quantification of ultrastructural features, electron micrographs were examined from 3 different animals
804 per treatment. The data were analysed using Student's t-test.

805 Bang Sensitivity
806 The bang sensitivity phenotype was tested after 1, 10 and 20 days of chronic exposure to 0.2 ppm
807 spinosad. Flies were vortexed on a VWR vortex at maximum strength for 10 s. The time required for
808 flies to flip over and regain normal standing posture was then recorded. The data were analysed using
809 Wilcoxon signed-rank test.
810
811 Climbing assay
812 Climbing phenotype was tested after 1, 10 and 20 days of exposure to 0.2 ppm spinosad. 5 adult
813 female flies were placed into a clean vial and allowed to rest for 30 min. Vials were tapped against a
814 pad and the time required for the flies to climb up to a pre-determined height (7 cm) was recorded.

Flies that did not climb the pre-determined height within 30 seconds were deemed to have failed the test. The data were analysed using Wilcoxon signed-rank test.

Graphs and Statistical analysis
All graphs were created, and all statistical analysis were performed in the software R (v.3.4.3). Images were designed using the free image software Inkscape (0.92.4).

Many of the analyses performed here were conducted on spinosad and imidacloprid in parallel with these treatments sharing the same controls, allowing direct comparison of the impact of these insecticides. The imidacloprid data were published in (Martelli et al., 2020). The data with shared controls are shown in Fig 1 (A,D,E), Fig 3 (A,B,C,D,E,F), Fig 4 (A,B,C), Fig 4 - figure supplement 1, Fig 4 - figure supplement 2 (D,E), Fig 4 - figure supplement 3, Fig 4 - figure supplement 4, Fig 5 (E), Fig 6, Fig 6 - table supplement 1, Fig 7 (B) and Fig 8 (C,D,E).

Acknowledgments:

Funding: F.M. was supported by a Victorian Latin America Doctoral Scholarship, an Alfred Nicholas Fellowship, a UoM Faculty of Science Travelling Scholarship, and The Robert Johanson and Anne Swann Fund - Native Animals Trust (awarded to F.M. and T.P). P.B. was supported by the University of Melbourne. H.J.B. was supported by the Howard Hughes Medical Institute (HHMI) and is an investigator of HHMI. K.V. was supported by NIH (NIA) grant. Lipid analysis were performed at Metabolomics Australia at University of Melbourne, which is a National Collaborative Research Infrastructure Strategy initiative under Bioplatforms Australia Pty Ltd (http://www.bioplatforms.com/).

Author Contribution: F.M., T.P., P.B. and H.J.B. conceived the study and designed the experiments. F.M. performed toxicology assays, all tissue confocal microscopy, behavioral assays, metabolic assays, and transcriptomics analysis. F.M. and Z.Z. processed and analysed the electron microscopy data. F.M. and J.W. performed the ERG analysis and RNAi experiments. F.M., T.R. and U.R. performed the lipidomic analysis. F.M., C.O.W., N.E.K. and K.V. performed GCaMP experiments. T.P., P.B. and H.J.B. acquired funding and supervised the research. F.M., P.B. and H.J.B. wrote the manuscript. All authors read, edited, reviewed, and approved the final version of the manuscript.

Competing interests: The authors confirm that there are no competing interests.

References

Aizen MA, Garibaldi LA, Cunningham SA, Klein AM. 2009. How much does agriculture depend on pollinators? Lessons from long-term trends in crop production. *Ann Bot* **103**:1579–1588. doi:10.1093/aob/mcp076

Bailey AP, Koster G, Guillermier C, Hirst EMA, MacRae JI, Lechene CP, Postle AD, Gould AP. 2015. Antioxidant Role for Lipid Droplets in a Stem Cell Niche of *Drosophila*. *Cell* **163**:340–353. doi:10.1016/j.cell.2015.09.020

Balieira KVB, Mazzo M, Bizerra PFV, Guimarães ARJS, Nicodemo D, Mingatto FE. 2018. Imidacloprid-induced oxidative stress in honey bees and the antioxidant action of caffeine. *Apidologie* **49**:562–572. doi:10.1007/s13592-018-0583-1

Biondi A, Mommaerts V, Smagghe G, Viñuela E, Zappalà L, Desneux N. 2012. The non-target impact of spinosyns on beneficial arthropods. *Pest Manag Sci* **68**:1523–1536. doi:10.1002/ps.3396

Buckingham SD, Lapied B, Le Corronc H, Grolleau F, Sattelle DB. 1997. Imidacloprid actions on insect neuronal acetylcholine receptors. *J Exp Biol* **200**:2685–2692.

Cardoso P, Barton PS, Birkhofer K, Chichorro F, Deacon C, Fartmann T, Fukushima CS, Gaigher R, Habel JC, Hallmann CA, Hill MJ, Hochkirch A, Kwak ML, Mammola S, Ari Noriega J, Orfinger AB, Pedraza F, Pryke JS, Roque FO, Settele J, Simaika JP, Stork NE, Suhling F, Vorster C, Samways MJ. 2020. Scientists' warning to humanity on insect extinctions. *Biol Conserv* **242**. doi:10.1016/j.biocon.2020.108426

Cheng YS, Zheng J, VanderGheynst JS. 2011. Rapid Quantitative Analysis of Lipids Using a Colorimetric Method in a Microplate Format. *Lipids* **46**:95–103. doi:10.1007/s11745-010-3494-0

Chmiel JA, Daisley BA, Burton JP, Reid G. 2019. Deleterious Effects of Neonicotinoid Pesticides on Drosophila melanogaster Immune Pathways. *MBio* **10**:1–14. doi:10.1128/mBio.01395-19

Chouhan AK, Guo C, Hsieh YC, Ye H, Senturk M, Zuo Z, Li Y, Chatterjee S, Botas J, Jackson GR, Bellen HJ, Shulman JM. 2016. Uncoupling neuronal death and dysfunction in Drosophila models of neurodegenerative disease. *Acta Neuropathol Commun* **4**:62. doi:10.1186/s40478-016-0333-4

Cleveland CB, Bormett GA, Saunders DG, Powers FL, McGibbon AS, Reeves GL, Rutherford L, Balcer JL. 2002. Environmental fate of spinosad. 1. Dissipation and degradation in aqueous systems. *J Agric Food Chem* **50**:3244–3256. doi:10.1021/jf011663i

Crouse GD, Demeter DA, Samaritoni G, McLeod CL, Sparks TC. 2018. De Novo Design of Potent, Insecticidal Synthetic Mimics of the Spinosyn Macrolide Natural Products. *Sci Rep* **8**:8–13. doi:10.1038/s41598-018-22894-6

Daniels RW, Rossano AJ, Macleod GT, Ganetzky B. 2014. Expression of multiple transgenes from a single construct using viral 2A peptides in *Drosophila*. *PLoS One* **9**. doi:10.1371/journal.pone.0100637

Darios F, Stevanin G. 2020. Impairment of Lysosome Function and Autophagy in Rare Neurodegenerative Diseases. *J Mol Biol* **432**:2714–2734. doi:10.1016/j.jmb.2020.02.033

Dawaliby R, Trubbia C, Delporte C, Noyon C, Ruysschaert JM, Van Antwerpen P, Govaerts C. 2016. Phosphatidylethanolamine is a key regulator of membrane fluidity in eukaryotic cells. *J Biol Chem* **291**:3658–3667. doi:10.1074/jbc.M115.706523

Denecke S, Nowell CJ, Fournier-Level A, Perry T, Batterham P. 2015. The wiggle index: An open source bioassay to assess sub-lethal insecticide response in *Drosophila melanogaster*. *PLoS One* **10**:1–18. doi:10.1371/journal.pone.0145051

Deus CM, Yambire KF, Oliveira PJ, Raimundo N. 2020. Mitochondria–Lysosome Crosstalk: From Physiology to Neurodegeneration. *Trends Mol Med* **26**:71–88. doi:10.1016/j.molmed.2019.10.009

Egea J, Buendia I, Parada E, Navarro E, León R, Lopez MG. 2015. Anti-inflammatory role of microglial alpha7 nAChRs and its role in neuroprotection. *Biochem Pharmacol* **97**:463–472. doi:10.1016/j.bcp.2015.07.032

Fergestad T, Bostwick B, Ganetzky B. 2006. Metabolic disruption in drosophila bang-sensitive seizure mutants. *Genetics* **173**:1357–1364. doi:10.1534/genetics.106.057463

Fusetto R, Denecke S, Perry T, O'Hair RAJ, Batterham P. 2017. Partitioning the roles of CYP6G1 and gut microbes in the metabolism of the insecticide imidacloprid in Drosophila melanogaster. *Sci Rep* **7**:1–12. doi:10.1038/s41598-017-09800-2

Gottlieb RA, Stotland A. 2015. MitoTimer: a novel protein for monitoring mitochondrial turnover in the heart. *J Mol Med* **93**:271–278. doi:10.1007/s00109-014-1230-6

Guan XL, Cestra G, Shui G, Kuhrs A, Schittenhelm RB, Hafen E, van der Goot FG, Robinett CC, Gatti M, Gonzalez-Gaitan M, Wenk MR. 2013. Biochemical Membrane Lipidomics during *Drosophila* Development. *Dev Cell* **24**:98–111. doi:10.1016/j.devcel.2012.11.012

Ioannou MS, Jackson J, Sheu SH, Chang CL, Weigel AV, Liu H, Pasolli HA, Xu CS, Pang S, Matthies D, Hess HF, Lippincott-Schwartz J, Liu Z. 2019. Neuron-Astrocyte Metabolic Coupling Protects against Activity-Induced Fatty Acid Toxicity. *Cell* **177**:1522-1535.e14. doi:10.1016/j.cell.2019.04.001

909 Karami-Mohajeri S, Abdollahi M. 2011. Toxic influence of organophosphate, carbamate, and
910 organochlorine pesticides on cellular metabolism of lipids, proteins, and carbohydrates: A
911 systematic review. *Hum Exp Toxicol* **30**:1119–1140. doi:10.1177/0960327110388959

912 Kerr JT. 2017. A Cocktail of Toxins. *Science* **356**:1331–1332. doi:10.1126/science.aan6713

913 Klein A-M, Vaissière BE, Cane JH, Steffan-Dewenter I, Cunningham SA, Kremen C, Tscharntke T.
914 2007. Importance of pollinators in changing landscapes for world crops. *Proc R Soc B Biol Sci*
915 **274**:303–313. doi:10.1098/rspb.2006.3721

916 Korolchuk VI, Menzies FM, Rubinsztein DC. 2010. Mechanisms of cross-talk between the ubiquitin-
917 proteasome and autophagy-lysosome systems. *FEBS Lett* **584**:1393–1398.
918 doi:10.1016/j.febslet.2009.12.047

919 Krahmer N, Guo Y, Wilfling F, Hilger M, Lingrell S, Heger K, Newman HW, Schmidt-supprian M,
920 Vance DE, Mann M, Farese RV, Walther TC. 2011. Phosphatidylcholine Synthesis for Lipid
921 Droplet Expansion Is Mediated by Localized Activation of CTP□: Phosphocholine
922 Cytidylyltransferase. *Cell Metab* **14**:504–515. doi:10.1016/j.cmet.2011.07.013

923 Liu L, Mackenzie K., Putluri N, Bellen HJ. 2017. The Glia-Neuron Lactate Shuttle and Elevated ROS
924 Promote Lipid Synthesis in Neurons and Lipid Droplet Accumulation in Glia via APOE / D Article
925 The Glia-Neuron Lactate Shuttle and Elevated ROS Promote Lipid Synthesis in Neurons and
926 Lipid Droplet Accumulat. *Cell Metab* 1–19. doi:10.1016/j.cmet.2017.08.024

927 Liu L, Zhang K, Sandoval H, Yamamoto S, Jaiswal M, Sanz E, Li Z, Hui J, Graham BH, Quintana A,
928 Bellen HJ. 2015. Glial lipid droplets and ROS induced by mitochondrial defects promote
929 neurodegeneration. *Cell* **160**:177–190. doi:10.1016/j.cell.2014.12.019

930 Lopes MP, Fernandes KM, Tomé HVV, Gonçalves WG, Miranda FR, Serrão JE, Martins GF. 2018.
931 Spinosad-mediated effects on the walking ability, midgut, and Malpighian tubules of Africanized
932 honey bee workers. *Pest Manag Sci* **74**:1311–1318. doi:10.1002/ps.4815

933 Lu C, Warchol KM, Callahan RA. 2014. Sub-lethal exposure to neonicotinoids impaired honey bees
934 winterization before proceeding to colony collapse disorder. *Bull Insectology* **67**:125–130.

935 Lukaszewicz-Hussain A. 2010. Role of oxidative stress in organophosphate insecticide toxicity - Short
936 review. *Pestic Biochem Physiol* **98**:145–150. doi:10.1016/j.pestbp.2010.07.006

937 Lundin O, Rundlöf M, Smith HG, Fries I, Bommarco R. 2015. Neonicotinoid insecticides and their
938 impacts on bees: A systematic review of research approaches and identification of knowledge
939 gaps. *PLoS One* **10**:1–20. doi:10.1371/journal.pone.0136928

940 Luo X, Rosenfeld JA, Yamamoto S, Harel T, Zuo Z, Hall M, Wierenga K, Pastore MT, Bartholomew D,
941 Delgado MR, Rotenberg J, Lewis RA, Emrick L, Bacino CA, Eldomery MK, Akdemir ZC, Xia F,
942 Yang Y, Lalani SR, Lotze T, Lupski JR, Lee B, Bellen HJ, Wangler MF. 2017. Clinically severe
943 CACNA1A alleles affect synaptic function and neurodegeneration differentially. *PLoS Genet* **13**.
944 doi:10.1371/journal.pgen.1006905

945 Martelli F, Zhongyuan Z, Wang J, Wong C-O, Karagas NE, Roessner U, Rupasinghe T,
946 Venkatachalam K, Perry T, Bellen HJ, Batterham P. 2020. Low doses of the neonicotinoid
947 insecticide imidacloprid induce ROS triggering neurological and metabolic impairments in
948 Drosophila . *Proc Natl Acad Sci* **117**:25840–25850. doi:10.1073/pnas.2011828117

949 McGurk L, Berson A, Bonini NM. 2015. Drosophila as an in vivo model for human neurodegenerative
950 disease. *Genetics* **201**:377–402. doi:10.1534/genetics.115.179457

951 Müller C. 2018. Impacts of sublethal insecticide exposure on insects — Facts and knowledge gaps.
952 *Basic Appl Ecol* **30**:1–10. doi:10.1016/j.baae.2018.05.001

953 Nguyen J, Ghazali R, Batterham P, Perry T. 2021. Inhibiting the proteasome reduces molecular and

biological impacts of the natural product insecticide, spinosad. *Pest Manag Sci* ps.6290. doi:10.1002/ps.6290

Owusu-Ansah E, Yavari A, Banerjee U. 2008. A protocol for in vivo detection of reactive oxygen species. *Nat Protoc* **doi:10.103**:1–10. doi:10.1038/nprot.2008.23

Perry T, Batterham P. 2018. Harnessing model organisms to study insecticide resistance. *Curr Opin Insect Sci* **27**:61–67. doi:10.1016/j.cois.2018.03.005

Perry T, Batterham P, Daborn PJ. 2011. The biology of insecticidal activity and resistance. *Insect Biochem Mol Biol* **41**:411–422. doi:10.1016/j.ibmb.2011.03.003

Perry T, Chen W, Ghazali R, Yang YT, Christesen D, Martelli F, Lumb C, Luong HNB, Mitchell J, Holien JK, Parker MW, Sparks TC, Batterham P. 2021. Role of nicotinic acetylcholine receptor subunits in the mode of action of neonicotinoid, sulfoximine and spinosyn insecticides in *Drosophila melanogaster. Insect Biochem Mol Biol. In press.*

Perry T, Heckel DG, McKenzie JA, Batterham P. 2008. Mutations in Dα1 or Dβ2 nicotinic acetylcholine receptor subunits can confer resistance to neonicotinoids in *Drosophila melanogaster*. *Insect Biochem Mol Biol* **38**:520–528. doi:10.1016/j.ibmb.2007.12.007

Perry T, McKenzie JA, Batterham P. 2007. A Dα6 knockout strain of Drosophila melanogaster confers a high level of resistance to spinosad. *Insect Biochem Mol Biol* **37**:184–188. doi:10.1016/j.ibmb.2006.11.009

Perry T, Somers J, Yang YT, Batterham P. 2015. Expression of insect α6-like nicotinic acetylcholine receptors in Drosophila melanogaster highlights a high level of conservation of the receptor: Spinosyn interaction. *Insect Biochem Mol Biol* **64**:106–115. doi:10.1016/j.ibmb.2015.01.017

Plotegher N, Duchen MR. 2017. Mitochondrial Dysfunction and Neurodegeneration in Lysosomal Storage Disorders. *Trends Mol Med* **23**:116–134. doi:10.1016/j.molmed.2016.12.003

Puinean AM, Lansdell SJ, Collins T, Bielza P, Millar NS. 2013. A nicotinic acetylcholine receptor transmembrane point mutation (G275E) associated with resistance to spinosad in Frankliniella occidentalis. *J Neurochem* **124**:590–601. doi:10.1111/jnc.12029

Quintana A, Kruse SE, Kapur RP, Sanz E, Palmiter RD. 2010. Complex I deficiency due to loss of Ndufs4 in the brain results in progressive encephalopathy resembling Leigh syndrome. *Proc Natl Acad Sci U S A* **107**:10996–11001. doi:10.1073/pnas.1006214107

Ren M, Phoon CKL, Schlame M. 2014. Metabolism and function of mitochondrial cardiolipin. *Prog Lipid Res*. doi:10.1016/j.plipres.2014.04.001

Saheki Y, De Camilli P. 2012. Synaptic Vesicle Endocytosis. *Cold Spring Harb Perspect Biol* **4**:a005645–a005645. doi:10.1101/cshperspect.a005645

Salgado VL. 1998. Studies on the Mode of Action of Spinosad: Insect Symptoms and Physiological Correlates. *Pestic Biochem Physiol* **60**:91–102.

Salgado VL, Saar R. 2004. Desensitizing and non-desensitizing subtypes of alpha-bungarotoxin-sensitive nicotinic acetylcholine receptors in cockroach neurons. *J Insect Physiol* **50**:867–879. doi:10.1016/j.jinsphys.2004.07.007

Sánchez-Bayo F, Wyckhuys KAG. 2019. Worldwide decline of the entomofauna: A review of its drivers. *Biol Conserv*. doi:10.1016/j.biocon.2019.01.020

Saras A, Tanouye MA. 2016. Mutations of the Calcium Channel Gene cacophony Suppress Seizures in Drosophila. *PLoS Genet* **12**:1–17. doi:10.1371/journal.pgen.1005784

996 Sattelle DB, Jones AK, Sattelle BM, Matsuda K, Reenan R, Biggin PC. 2005. Edit, cut and paste in
997 the nicotinic acetylcholine receptor gene family ofDrosophila melanogaster. *BioEssays* **27**:366–
998 376. doi:10.1002/bies.20207

999 Schürmann FW. 2016. Fine structure of synaptic sites and circuits in mushroom bodies of insect
1000 brains. *Arthropod Struct Dev* **45**:399–421. doi:10.1016/j.asd.2016.08.005

1001 Somers J, Nguyen J, Lumb C, Batterham P, Perry T. 2015. In vivo functional analysis of the
1002 Drosophila melanogaster nicotinic acetylcholine receptor Dα6 using the insecticide spinosad.
1003 *Insect Biochem Mol Biol* **64**:116–127. doi:10.1016/j.ibmb.2015.01.018

1004 Sparks TC, Hahn DR, Garizi N V. 2017. Natural products, their derivatives, mimics and synthetic
1005 equivalents: role in agrochemical discovery. *Pest Manag Sci* **73**:700–715. doi:10.1002/ps.4458

1006 Stepien KM, Roncaroli F, Turton N, Hendriksz CJ, Roberts M, Heaton RA, Hargreaves I. 2020.
1007 Mechanisms of Mitochondrial Dysfunction in Lysosomal Storage Disorders: A Review. *J Clin*
1008 *Med* **9**:2596. doi:10.3390/jcm9082596

1009 Terhzaz S, Cabrero P, Brinzer RA, Halberg KA, Dow JAT, Davies S. 2015. A novel role of *Drosophila*
1010 cytochrome P450-4e3 in permethrin insecticide tolerance. *Insect Biochem Mol Biol* **67**:38–46.
1011 doi:10.1016/j.ibmb.2015.06.002

1012 Tosi S, Costa C, Vesco U, Quaglia G, Guido G. 2018. A 3-year survey of Italian honey bee-collected
1013 pollen reveals widespread contamination by agricultural pesticides. *Sci Total Environ* **615**:208–
1014 218. doi:10.1016/j.scitotenv.2017.09.226

1015 Valko M, Leibfritz D, Moncol J, Cronin MTD, Mazur M, Telser J. 2007. Free radicals and antioxidants
1016 in normal physiological functions and human disease. *Int J Biochem Cell Biol* **39**:44–84.
1017 doi:10.1016/j.biocel.2006.07.001

1018 van Klink R, Bowler DE, Gongalsky KB, Swengel AB, Gentile A, Chase JM. 2020. Meta-analysis
1019 reveals declines in terrestrial but increases in freshwater insect abundances. *Science (80-)*
1020 **420**:in press. doi:10.1126/science.aax9931

1021 Wagner DL, Grames EM, Forister ML, Berenbaum MR, Stopak D. 2021. Insect decline in the
1022 Anthropocene: Death by a thousand cuts. *Proc Natl Acad Sci U S A* **118**:1–10.
1023 doi:10.1073/pnas.2023989118

1024 Wang T, Montell C. 2007. Phototransduction and retinal degeneration in *Drosophila*. *Pflugers Arch*
1025 *Eur J Physiol* **454**:821–847. doi:10.1007/s00424-007-0251-1

1026 Wang X, Martínez MA, Dai M, Chen D, Ares I, Romero A, Castellano V, Martínez M, Rodríguez JL,
1027 Martínez-Larrañaga MR, Anadón A, Yuan Z. 2016. Permethrin-induced oxidative stress and
1028 toxicity and metabolism. A review. *Environ Res*. doi:10.1016/j.envres.2016.05.003

1029 Watson GB. 2001. Actions of Insecticidal Spinosyns on γ-Aminobutyric Acid Responses from Small-
1030 Diameter Cockroach Neurons. *Pestic Biochem Physiol* **71**:20–28. doi:10.1006/pest.2001.2559

1031 Watson GB, Chouinard SW, Cook KR, Geng C, Gifford JM, Gustafson GD, Hasler JM, Larrinua IM,
1032 Letherer TJ, Mitchell JC, Pak WL, Salgado VL, Sparks TC, Stilwell GE. 2010. A spinosyn-
1033 sensitive Drosophila melanogaster nicotinic acetylcholine receptor identified through chemically
1034 induced target site resistance, resistance gene identification, and heterologous expression.
1035 *Insect Biochem Mol Biol* **40**:376–384. doi:10.1016/j.ibmb.2009.11.004

1036 Weber AL, Khan GF, Magwire MM, Tabor CL, Mackay TFC, Anholt RRH. 2012. Genome-wide
1037 association analysis of oxidative stress resistance in drosophila melanogaster. *PLoS One* **7**.
1038 doi:10.1371/journal.pone.0034745

1039 Wong CO, Chen K, Lin YQ, Chao Y, Duraine L, Lu Z, Yoon WH, Sullivan JM, Broadhead GT, Sumner
1040 CJ, Lloyd TE, Macleod GT, Bellen HJ, Venkatachalam K. 2014. A TRPV channel in drosophila

motor neurons regulates presynaptic resting Ca2+ levels, synapse growth, and synaptic transmission. *Neuron* **84**:764–777. doi:10.1016/j.neuron.2014.09.030

Wu-Smart J, Spivak M. 2016. Sub-lethal effects of dietary neonicotinoid insecticide exposure on honey bee queen fecundity and colony development. *Sci Rep* **6**:1–11. doi:10.1038/srep32108

Xu W, Yang M, Gao J, Zhang Y, Tao L. 2018. Oxidative stress and DNA damage induced by spinosad exposure in spodoptera frugiperda Sf9 cells. *Food Agric Immunol* **29**:171–181. doi:10.1080/09540105.2017.1364708

Yambire KF, Mosquera LF, Steinfeld R, Mühle C, Ikonen E, Milosevic I, Raimundo N. 2018. Mitochondrial biogenesis is transcriptionally repressed in lysosomal lipid storage diseases. *bioRxiv* 1–29. doi:10.1101/381376

Yan LJ, Levine RL, Sohal RS. 1997. Oxidative damage during aging targets mitochondrial aconitase. *Proc Natl Acad Sci U S A* **94**:11168–11172.

Yang M, Wang B, Gao J, Zhang Y, Xu W, Tao L. 2017. Spinosad induces programmed cell death involves mitochondrial dysfunction and cytochrome C release in Spodoptera frugiperda Sf9 cells. *Chemosphere* **169**:155–161. doi:10.1016/j.chemosphere.2016.11.065

1076

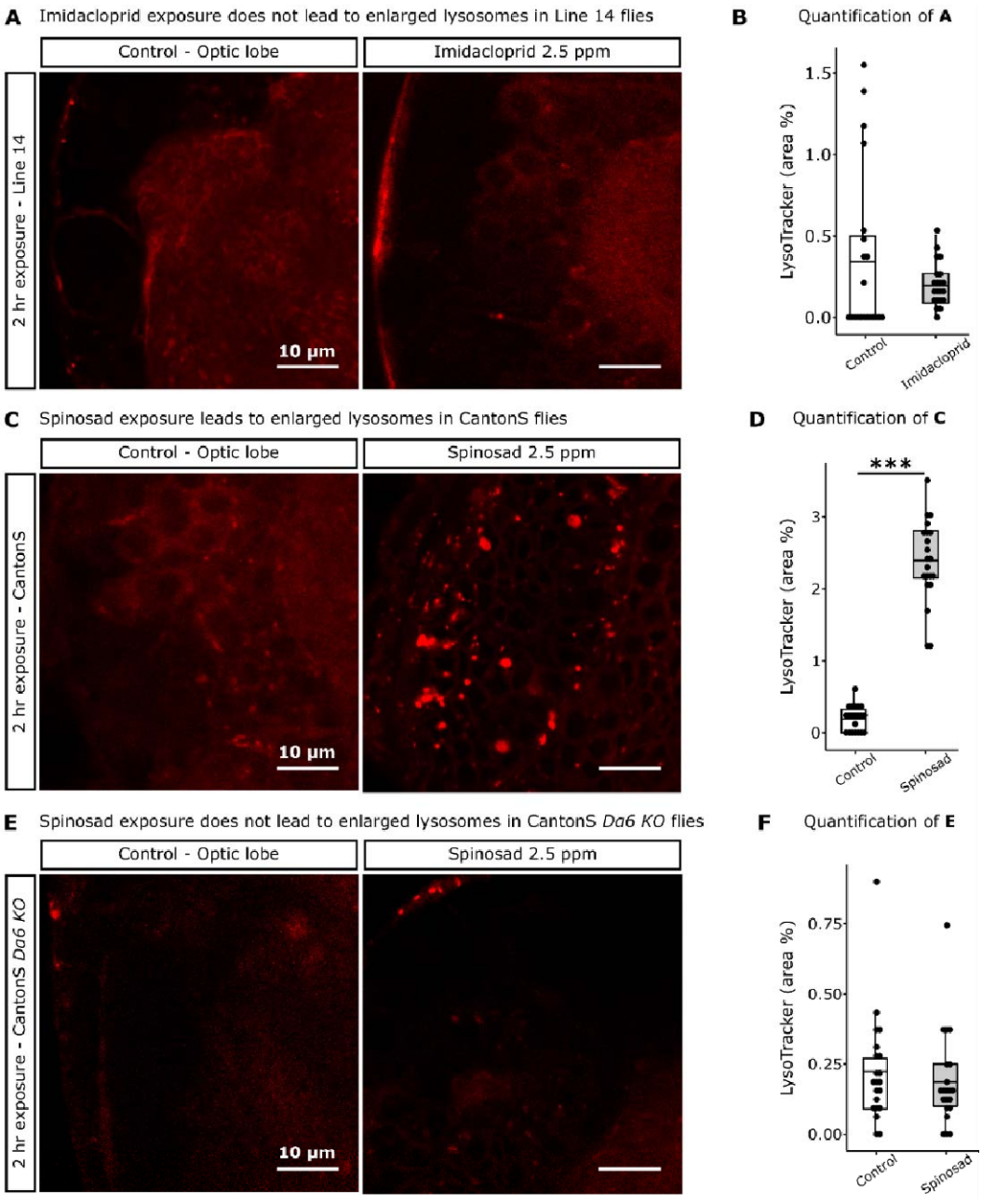

1077

1078 **Figure 2 – figure supplement 1. Enlarged lysosomes are only observed in response to**
1079 **spinosad exposure and in the presence of Dα6 nAChRs. A,** Line 14 larvae exposed to 2.5 ppm
1080 imidacloprid for 2hr show no enlarged lysosomes in the brain. **B,** Quantification of A, LysoTracker
1081 area in the optic lobes (%) (n = 7 larvae/treatment, 3 optic lobe sections/larva). **C,** CantonS larvae
1082 exposed to 2.5 ppm spinosad for 2hr show significant increase in the number of enlarged lysosomes
1083 in the brain. **D,** Quantification of C, LysoTracker area in the optic lobes (%) (n = 7 larvae/treatment, 3
1084 optic lobe sections/larva). **E,** CantonS *Dα6 knockout* larvae exposed to 2.5 ppm spinosad for 2hr
1085 show no enlarged lysosomes in the brain. **F,** Quantification of E, LysoTracker area in the optic lobes
1086 (%) (n = 7 larvae/treatment, 3 optic lobe sections/larva). Lysotracker staining, 400 x magnification.
1087 Microscopy images obtained in Leica SP5 Laser Scanning Confocal Microscope. t-test; ***P < 0.001.

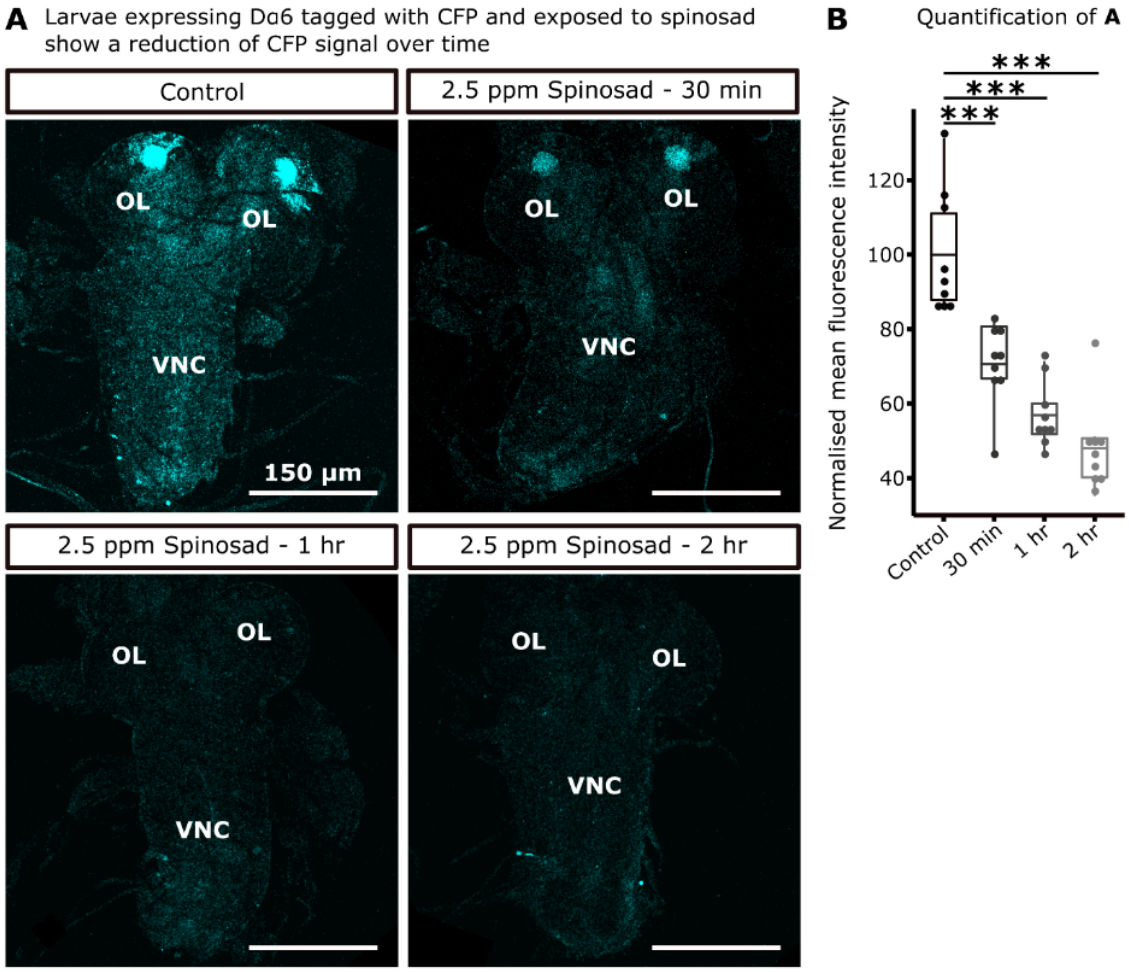

Figure 2 – figure supplement 2. Exposure to spinosad reduces Dα6 nAChRs in neuronal membranes. A, Brains from larvae obtained by crossing UAS Dα6 CFP tagged in Line 14 *Dα6 KO* strain to Gal4-L driver in Line 14 *Dα6 KO* strain were exposed to 2.5 ppm spinosad for 30 min, 1 hr or 2 hr. **B,** Quantification of **A** (n = 3 larvae/condition, 3 brain sections/larva). Microscopy images obtained in Leica SP5 Laser Scanning Confocal Microscope, 400 x magnification. OP – optic lobe; VNC – ventral nerve cord. t-test; ***P < 0.001.

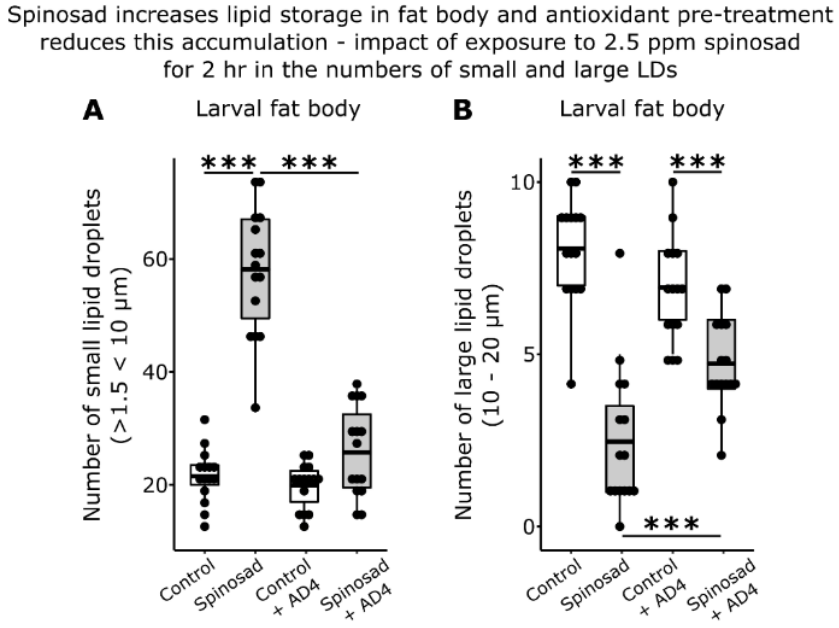

Figure 4 – figure supplement 1. Impact of spinosad exposure on LD dynamics in fat body. Larvae exposed to 2.5 ppm spinosad for 2 hr show an accumulation of small LDs and reduction of large LD in the fat body. 5 hr pre-treatment with 300 µg/mL of antioxidant N-acetylcysteine amide (NACA) reduces this effect. **A,** Number of small LD (> 1.5 µm < 10 µm)**. B,** Number of large LD (10 µm - 20 µm). n = 3 larvae/group; 5 image sections/larva. t-test; ***P < 0.001.

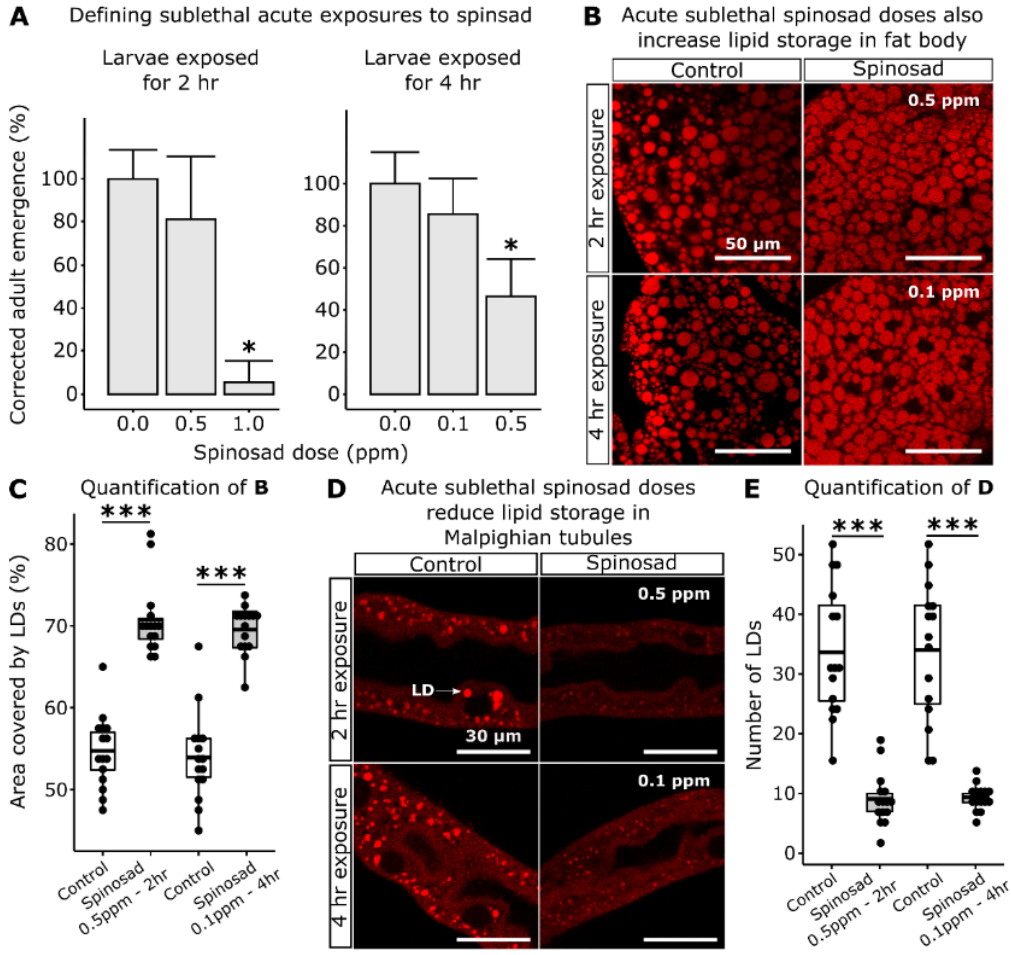

Figure 4 – figure supplement 2. Spinosad doses that do not affect survival impact the larval lipid environment. A, Corrected adult emergence relative to controls - larvae exposed to different spinosad doses were rinsed in 5% sucrose and placed back onto insecticide-free media for quantification of adult emergence. 0.5 ppm for 2 hr and 0.1 ppm for 4 hr were determined as the highest doses that do not affect survival. **B,** Accumulation of LD in the fat body of larvae in response to the highest doses that do not affect survival. **C,** Percentage of area occupied by LD in fat body (n = 3 larvae/treatment; 5 image sections/larva). **D,** Reduction of lipid storage in Malpighian tubules of larvae exposed to the highest doses that do not affect survival. White arrow indicates a LD. **E,** Number of lipid droplets per Malpighian Tubule (n = 3 larvae/treatment; 5 sections/larva). Microscopy images obtained in Leica SP5 Laser Scanning Confocal Microscope, 400x magnification, Nile red staining. Error bars in **A** indicate 95% confidence interval (One-way ANOVA, Turkey's HSD; *P < 0.05). **C** and **E**, t-test; ***P < 0.001.

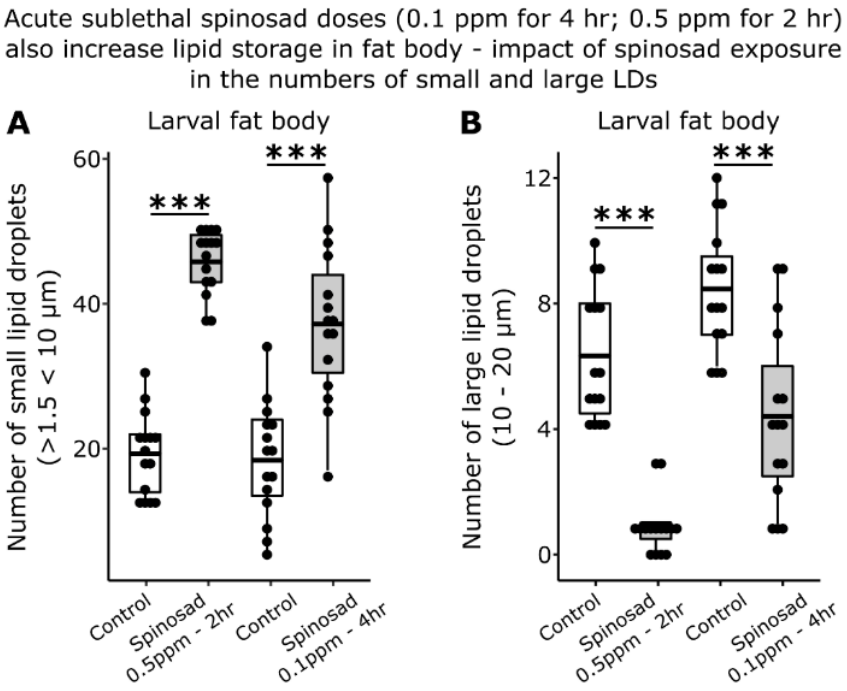

Figure 4 – figure supplement 3. The highest spinosad doses that do not affect survival also impact LD dynamics in fat body. Larvae exposed to 0.5 ppm spinosad for 2 hr, or 0.1 ppm spinosad for 4 hr, show an accumulation of small LD and reduction of large LD in the fat body. **A,** Number of small LD (> 1.5 µm < 10 µm)**. B,** Number of large LD (10 µm - 20 µm). n = 3 larvae/group; 5 image sections/larva. t-test; ***P < 0.001.

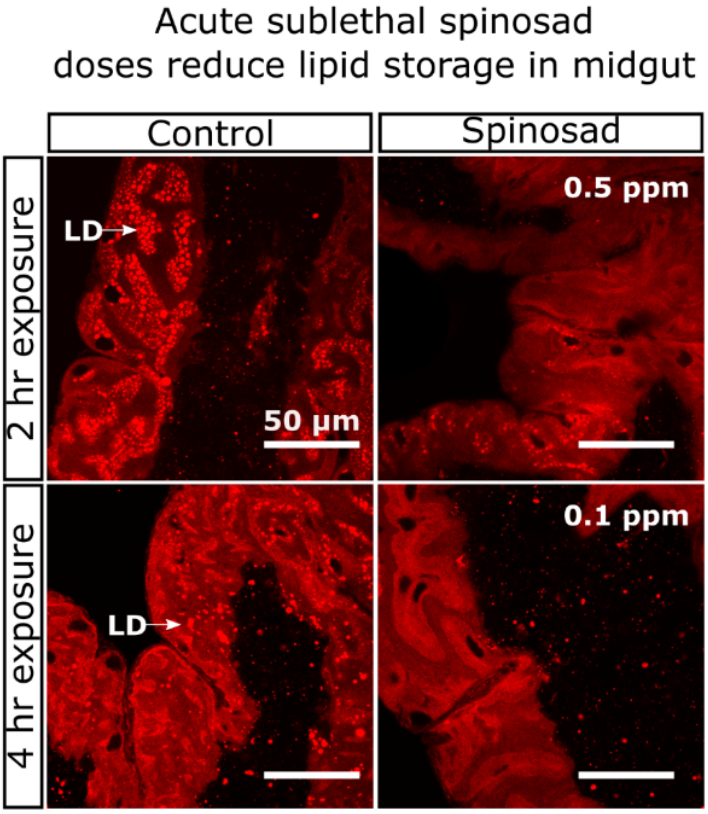

Figure 4 – figure supplement 4. Spinosad doses that do not affect survival impact the larval lipid environment. Posterior midgut. White arrow indicates a cluster of LDs. Zones with LD accumulation were not quantified since they were only found in non-exposed animals (n = 3 larvae/ treatment). Microscopy images obtained in Leica SP5 Laser Scanning Confocal Microscope, 400x magnification, Nile red staining.

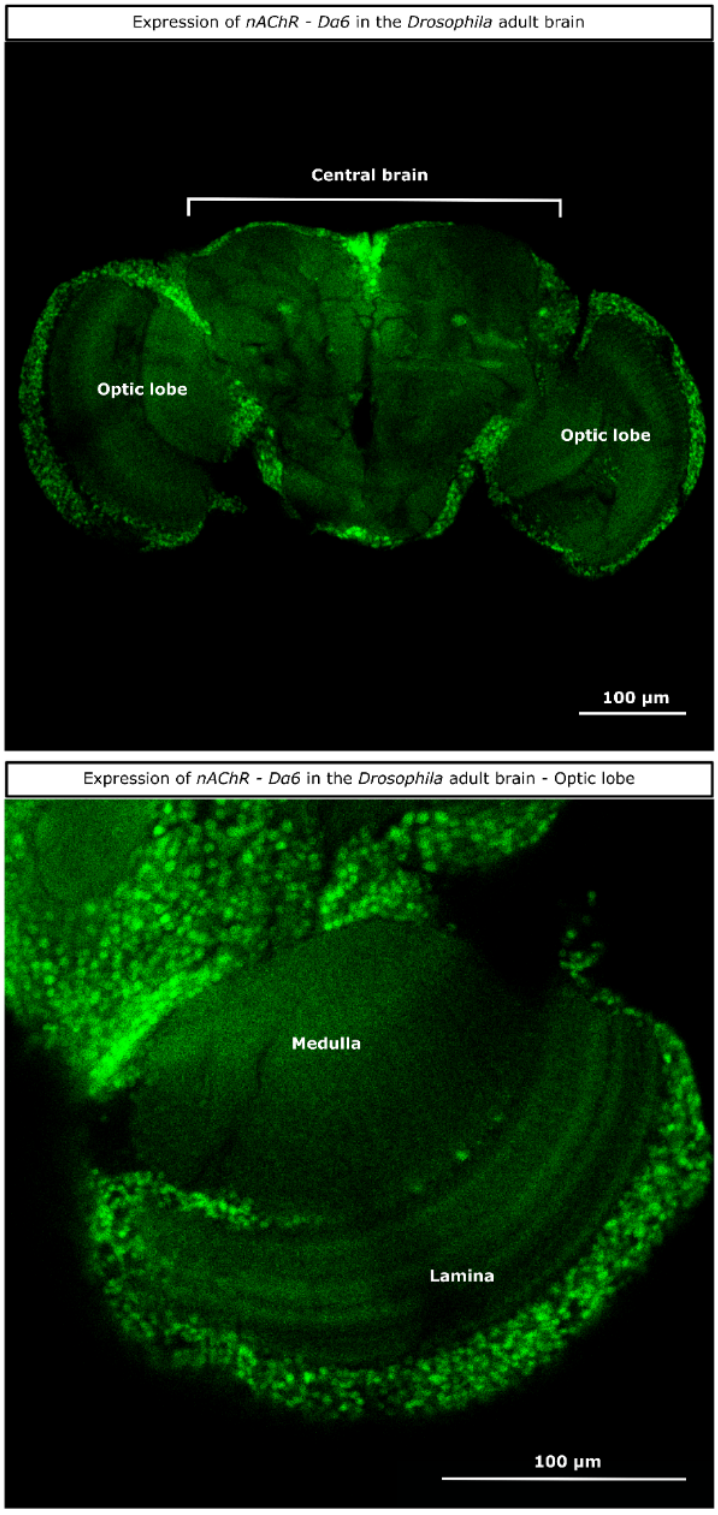

Figure 8 – figure supplement 1. Expression pattern of nAChR subunit *Dα6* in the *Drosophila* adult brain (*Dα6* T2A Gal4 > UAS-GFP.nls). Detail of the expression in lamina and medulla (optic lobe). Microscopy images obtained in Leica SP5 Laser Scanning Confocal Microscope. 400 x magnification.

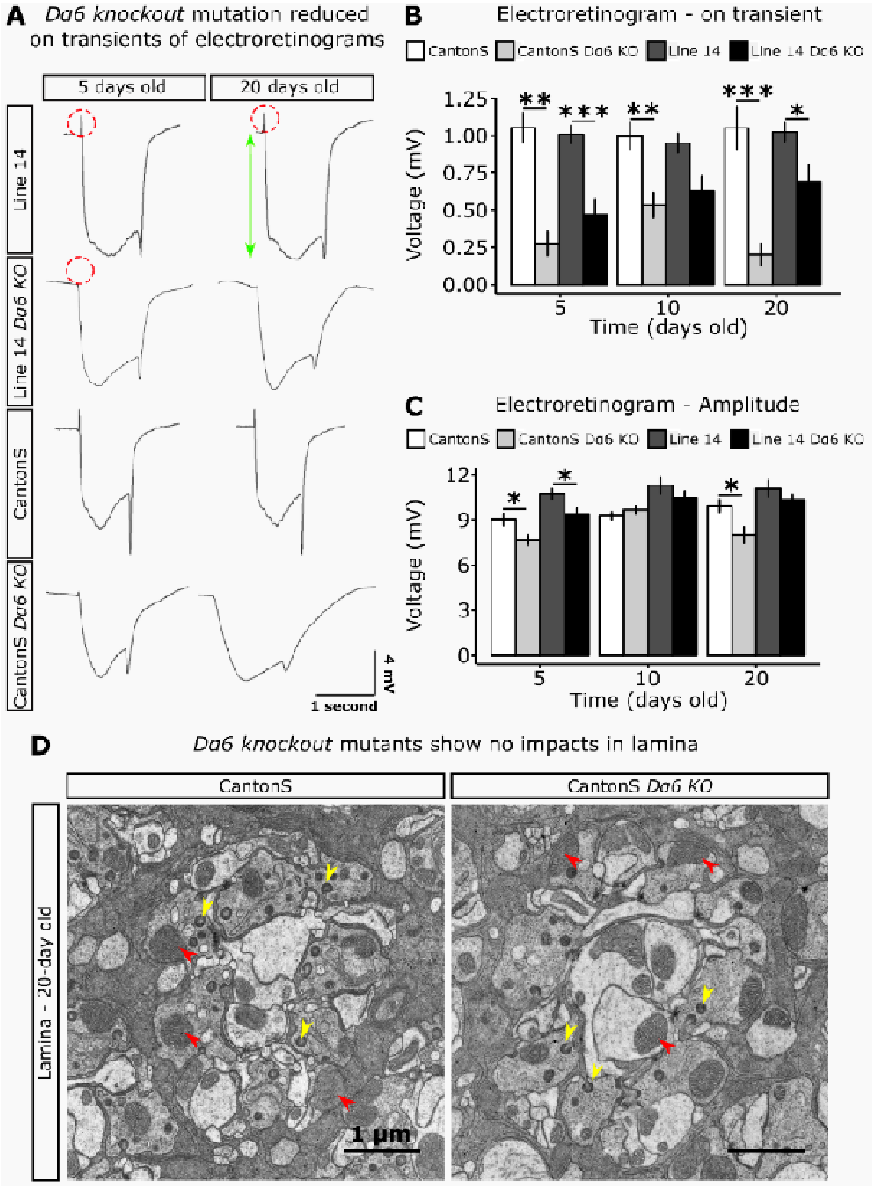

Figure 9 – figure supplement 1. nAChR *Dα6 knockout* (*KO*) mutants show defective electroretinograms (ERGs) but no damage in lamina. A, ERGs of 5- and 20-days old females from Line 14, Line 14 *Dα6 KO* mutant, Canton S and Canton S *Dα6 KO* mutant. Red dotted circles indicate the on-transient signal and green arrow indicates the amplitude (n = 8 to 10 adult flies/strain/time point) **B,** On-transient signal of ERGs of 5-, 10- and 20-days old flies. **C,** Amplitude of ERGs of 5-, 10- and 20-days old flies. **D,** Electron microscopy of the lamina of 20-day old Canton S and Canton S *Dα6 KO* mutant flies aged in the absence of spinosad. Red arrowheads indicate normal mitochondria, yellow arrowheads indicate capitate projections. No conspicuous difference was noticed between mutant and background strains (10 images/fly; 3 flies/genotype). t-test; *P < 0.05, **P < 0.01, ***P < 0.001.

1185

1186 **Figure 6 – table supplement 1. Impact of spinosad on the lipidomic profile.** Lipidomic profile of
1187 larvae exposed to 2.5 ppm spinosad or control (equivalent dose of DMSO) for 2 hr as detected by LC-
1188 MS. Values are expressed as peak intensity area normalized to sample weight.

Lipid species	Control 1	Control 2	Control 3	Spinosad 1	Spinosad 2	Spinosad 3	ANOVA, Tukey's HSD p-adj	F-value
2HPOT keto 34:2-PE-/16:0	123795.62	163589.74	219673.91	217767.86	176250	175247.52	0.5419233	0.443
2HPOT keto 34:2-PG-/16:0	90656.9	67008.5	89021.7	104107.1	117589.3	76435.6	0.2970207	1.435
2HPOT keto 34:3-PC-/16:0	77372.3	33076.9	58043.5	41875	42589.3	55247.5	0.5176349	0.502
2HPOT keto 34:3-PE-/16:0	933065.69	952820.51	1215326.1	1248660.7	1132232.1	1204851.5	0.1715842	2.767
2HPOT keto 34:3-PG-/16:0	778321.2	873846.2	713152.2	958750	810982.1	959703	0.1486808	3.189
2HPOT keto 36:4-PC-/2HPOT keto 36:4	754744.5	938119.7	916087	849821.4	981875	931584.2	0.4999316	0.549
2HPOT keto 36:4-PE-/18:1	2131167.9	2425726.5	2663478.3	2802767.9	2864107.1	3127920.8	0.0458895	8.185
2HPOT keto 36:4-PE-/18:2	1160292	1192649.6	1200434.8	1141696.4	1364821.4	1291485.1	0.2892342	1.490
2HPOT keto 36:4-PG-/18:1	1165255.5	1236239.3	1200108.7	1235000	1367410.7	1312079.2	0.07464646	5.743
2HPOT keto 36:4-PG-/18:2	667737.2	667435.9	531521.7	607232.1	672142.9	596534.7	0.9549847	0.004
2HPOT keto 36:5-PC-/18:3	680438	810940.2	648260.9	814821.4	845357.1	599108.9	0.6872676	0.188
2HPOT keto 36:5-PE-/18:2	488905.11	508205.13	590434.78	505625	610803.57	570297.03	0.4911734	0.573
2HPOT keto 36:5-PG-/18:2	271678.8	318461.5	243152.2	339107.1	371071.4	333267.3	0.04814691	7.916
2HPOT keto 36:6-PC-/18:3	51824.8	27094	31521.7	25267.9	65178.6	50297	0.5080307	0.527
CE 14:0	146788.3	242136.8	283695.7	45982.1	69464.3	39207.9	0.01419808	17.270
CE 16:0	188102.2	186153.8	236195.7	359285.7	233035.7	312475.2	0.07171429	5.922
CE 16:1	725912.4	732393.2	986195.7	524732.1	756964.3	828910.9	0.4255195	0.786
CE 18:1	3085839.4	3167435.9	3113043.5	3207500	1493482.1	3164158.4	0.4256607	0.785
CE 18:2	9927	79059.8	35978.3	20000	73928.6	35148.5	0.9601355	0.003
CL 62:3	37606.838	41282.051	23152.174	19107.143	7232.1429	3564.3564	0.02952137	10.990
CL 64:3	152820.51	159059.83	116304.35	65625	39553.571	22376.238	0.00544154	29.900
CL 64:4	1155726.5	1217948.7	898260.87	609642.86	283660.71	155940.59	0.01131725	19.730
CL 64:6	20341.88	18717.949	34239.13	23303.571	23392.857	16732.673	0.5750357	0.372
CL 65:0	10341.88	13589.744	11847.826	9375	11071.429	13465.347	0.7017686	0.169
CL 66:0	12478.632	12905.983	10000	10446.429	12946.429	10396.04	0.6892719	0.185
CL 66:3	101538.46	129487.18	48152.174	8482.1429	8125	14059.406	0.02580067	11.980
CL 66:4	575811.97	634786.32	513260.87	329017.86	146250	69702.97	0.009676818	21.600
CL 66:6	44017.094	35470.085	30760.87	28303.571	13125	6831.6832	0.05036087	7.670
CL 67:0	123247.86	114358.97	86413.043	55982.143	22767.857	19504.951	0.009472268	21.870
CL 68:10	36495.727	32649.573	34347.826	31875	32589.286	25247.525	0.1506398	3.149
CL 68:11	19743.59	23931.624	12934.783	3214.2857	4375	594.05941	0.008930132	22.620
CL 68:3	24871.795	21111.111	23913.043	15535.714	25000	13267.327	0.2274407	2.029

CL 68:4	90854.701	82564.103	43695.652	13214.286	16339.286	13861.386	0.01647519	15.800
CL 68:6	1092222.2	1137692.3	817934.78	269553.57	172410.71	111881.19	0.001638514	57.190
CL 69:0	636495.73	660000	430108.7	88303.571	80892.857	60891.089	0.002459115	46.080
CL 70:0	62136.752	79914.53	57173.913	58392.857	73571.429	54059.406	0.6536651	0.234
CL 70:10	111880.34	130085.47	100326.09	111785.71	111428.57	89108.911	0.4324939	0.760
CL 70:2	97179.487	114871.79	105652.17	106160.71	117321.43	89009.901	0.8664366	0.032
CL 70:4	5811.9658	14102.564	13369.565	8839.2857	12946.429	7821.7822	0.7108664	0.159
CL 70:6	113675.21	110512.82	45760.87	8571.4286	14464.286	19702.97	0.02761109	11.470
CL 72:10	30427.35	39658.12	21521.739	17321.429	15625	30693.069	0.2582735	1.734
CL 72:11	52307.692	75555.556	58260.87	46250	52232.143	50891.089	0.1642574	2.892
CL 72:4	214871.79	201452.99	188913.04	183125	198214.29	152574.26	0.1969343	2.391
CL 74:7	100341.88	94957.265	50217.391	68839.286	63125	35544.554	0.2413577	1.888
DG 28:0 -(14:0)	41232263	43517778	56964783	48507232	51229643	39195248	0.8867293	0.023
DG 30:0 -(14:0)	20333869	16738120	33330544	35592321	31987768	26947426	0.2262944	2.041
DG 30:0 -(15:0)	222116.8	189145.3	224782.6	84910.7	263125	203861.4	0.6286463	0.273
DG 30:0 -(16:0)	31792482	28049829	52891848	46444821	47469464	38735743	0.4640578	0.654
DG 30:1 -(14:0)	112222774	95524615	144444891	135975089	129559554	93132277	0.9176174	0.012
DG 30:1 -(14:1)	13757883	11986325	20162065	16855982	15285268	12458911	0.8838297	0.024
DG 30:1 -(16:0)	12133212	11247180	18532283	15314375	13634464	10981980	0.8132627	0.064
DG 30:1 -(16:1)	141050292	119525299	179823044	164481964	152594286	117753762	0.9383107	0.007
DG 32:0 -(14:0)	1981678.8	2075042.7	2994347.8	2233750	2945982.1	2221881.2	0.7858322	0.084
DG 32:0 -(16:0)	28784891	24649402	42998804	38700089	35333304	30870198	0.6625472	0.221
DG 32:0 -(18:0)	4620875.9	3709059.8	6845978.3	6595178.6	5694732.1	5813465.3	0.3728798	1.005
DG 32:1 -(14:0)	119655329	117577436	153631848	146367500	136873125	118173960	0.8181483	0.060
DG 32:1 -(14:1)	1084744.5	1191111.1	2034456.5	1757053.6	1613750	1260891.1	0.7648967	0.102
DG 32:1 -(16:0)	93221387	88162821	125805978	119928393	110233036	87595347	0.8280745	0.054
DG 32:1 -(16:1)	112397080	104677350	148316522	139003393	124129732	102728515	0.9931095	0.000
DG 32:1 -(18:0)	892335.8	1543418.8	2525978.3	2191607.1	1834732.1	1679505	0.6448556	0.248
DG 32:1 -(18:1)	137173577	129496667	183220326	171838125	156348125	127531980	0.9314351	0.008
DG 32:2 -(14:0)	8099197.1	7010427.4	9596304.3	8794107.1	9024553.6	6243069.3	0.8626771	0.034
DG 32:2 -(14:1)	16463504	14628974	23230109	20327679	18999107	14671881	0.9740802	0.001
DG 32:2 -(16:1)	204709270	186125812	293435000	296117857	290351339	218629703	0.3861522	0.945
DG 32:2 -(18:1)	13110438	11873162	17568261	17448482	14924643	13072574	0.6761583	0.202
DG 32:2 -(18:2)	12836788	11616068	18780326	13928304	15833839	9151980.2	0.6536608	0.234
DG 34:0 -(14:0)	180729.9	139743.6	273369.6	163928.6	226339.3	141089.1	0.6807093	0.196
DG 34:0 -(16:0)	5460729.9	4198547	7729239.1	7772678.6	7168303.6	5416435.6	0.4733192	0.625
DG 34:0 -(18:0)	6165255.5	4886837.6	9138369.6	8686607.1	8398571.4	7318019.8	0.34947	1.121
DG 34:0 -(20:0)	236496.4	342649.6	233587	268928.6	169732.1	255544.6	0.4520102	0.693
DG 34:1 -(16:1)	9410802.9	5651282.1	12105761	13179107	11926964	8892475.2	0.3713354	1.012

DG 34:1 -(18:0)	7627445.3	4759401.7	7893369.6	7157678.6	7296517.9	8465445.5	0.4631568	0.657
DG 34:1 -(18:1)	167782993	140669658	246624239	242133214	237998482	200824455	0.2893835	1.489
DG 34:1 -(20:0)	131751.8	324615.4	272826.1	253303.6	267142.9	357326.7	0.4960737	0.559
DG 34:2 -(16:0)	8007518.2	6161880.3	9911739.1	7007232.1	8140446.4	6580891.1	0.542135	0.443
DG 34:2 -(16:1)	84736861	76823846	118052283	114529911	111164911	92316535	0.4242981	0.790
DG 34:2 -(18:1)	139355183	128887265	202773261	202966696	184341429	158678317	0.397652	0.895
DG 34:2 -(18:2)	10302044	8617435.9	13534022	11898839	12304911	8522970.3	0.9636001	0.002
DG 36:0 -(16:0)	188102.2	186153.8	236195.7	359285.7	235535.7	286831.7	0.08372604	5.251
DG 36:0 -(18:0)	1768759.1	1696837.6	2512173.9	1393660.7	1547053.6	1807920.8	0.2270012	2.034
DG 36:0 -(20:0)	269416.1	275213.7	423804.3	351160.7	163928.6	172970.3	0.3032436	1.393
DG 36:1 -(16:1)	725912.4	732393.2	986195.7	524732.1	756964.3	828910.9	0.4255195	0.786
DG 36:1 -(18:0)	8194452.6	3938803.4	14448696	12242500	9150446.4	9168415.8	0.7015448	0.170
DG 36:1 -(18:1)	10549781	11541026	15197283	15342411	13948036	11321980	0.5795313	0.363
DG 36:1 -(20:0)	800875.9	728547	360000	1111517.9	932500	912970.3	0.07718021	5.597
DG 36:2 -(18:0)	999051.1	484017.1	1448913	1336250	1281250	828019.8	0.623064	0.283
DG 36:2 -(18:1)	37264964	35416752	49351413	44835804	39012143	38627030	0.9770349	0.001
DG 36:2 -(18:2)	800583.9	786752.1	1056195.7	1178928.6	848928.6	973168.3	0.4116126	0.839
DG 36:3 -(16:0)	12043.8	25555.6	0	9017.9	11607.1	0	0.5270203	0.479
DG 36:3 -(18:0)	146131.4	88547	71630.4	89107.1	100178.6	81980.2	0.6405598	0.254
DG 36:3 -(18:1)	4758467.2	4183418.8	4991304.3	3499107.1	3485089.3	3721584.2	0.01296218	18.220
DG 36:3 -(18:2)	5452335.8	4341111.1	6264891.3	4566785.7	4248303.6	3911584.2	0.1323347	3.558
DG 36:3 -(18:3)	128686.1	168803.4	82173.9	41875	121785.7	81584.2	0.2584312	1.733
DG 36:4 -(18:1)	304452.6	177265	181304.3	261339.3	462232.1	373861.4	0.1130596	4.094
DG 36:4 -(18:2)	1052992.7	797008.5	930652.2	860535.7	743750	621485.1	0.1413992	3.345
DG 36:4 -(18:3)	409051.1	301965.8	489565.2	294464.3	512053.6	334455.4	0.8289335	0.053
DG 38:1 -(18:1)	3085839.4	3167435.9	3113043.5	3207500	1493482.1	3164158.4	0.4256607	0.785
DG 38:1 -(20:0)	680948.9	401367.5	922391.3	841339.3	1216517.9	864950.5	0.1886158	2.506
DG 38:4 -(20:3)	27226.3	15042.7	17391.3	9017.9	0	0	0.02438948	12.410
DG 38:5 -(16:0)	14306.6	28290.6	27826.1	27410.7	15357.1	0	0.3712702	1.012
DG 38:5 -(20:3)	166642.3	108803.4	97826.1	78750	146785.7	159505	0.9109031	0.014
DG 38:5 -(22:5)	47080.3	27179.5	35760.9	15089.3	4017.9	19703	0.03276297	10.270
DG 38:6 -(16:0)	464525.5	914359	253152.2	330446.4	512053.6	176633.7	0.4012172	0.880
DG 38:6 -(22:5)	7299.3	20341.9	49021.7	21071.4	0	5940.6	0.2974293	1.433
dhCer 16:0	259416.1	110427.4	237826.1	239285.7	158035.7	0	0.4520158	0.693
dhCer 18:0	27810.2	26410.3	13152.2	34642.9	60982.1	33366.3	0.1127667	4.103
dhCer 20:0	18832.1	47350.4	2934.8	0	84107.1	13762.4	0.7584759	0.108
HOD 34:2-PC-/16:0	874160.6	350854.7	220869.6	107232.1	606517.9	393465.3	0.6708059	0.210
HOD 34:3-PC-/16:0	20799051	20560769	20739457	19178214	18878214	18728218	0.0002974	138.700
HOD 34:3-PE-/16:0	50000	66581.2	12608.7	15625	41517.9	39802	0.5829498	0.356

HOD 34:3-PG-/HOT 34:2 PG	163503.6	172051.3	45434.8	97767.9	84464.3	77920.8	0.3843419	0.953
HOD 36:4-PC-/18:1	1337518.2	1207777.8	1465108.7	994732.1	1312946.4	821188.1	0.1439454	3.289
HOD 36:4-PC-/18:2	1069854	672393.2	978478.3	322232.1	762321.4	464356.4	0.0917021	4.881
HOD 36:4-PE-/18:1	55401.5	81794.9	18260.9	41785.7	18750	52970.3	0.5419486	0.443
HOD 36:4-PG-/18:1	643211.7	651453	213913	319642.9	365714.3	391584.2	0.3802321	0.971
HOD 36:5-PC-/18:2	5985.4	4529.9	652.2	1964.3	3660.7	6633.7	0.8706898	0.030
HOD 36:5-PC-/18:3	374890.5	550256.4	403260.9	479642.9	464196.4	567920.8	0.3884604	0.934
HOD 36:5-PG-/HOT 36:4 PG	89854	52564.1	37391.3	35267.9	38125	39405.9	0.2262988	2.041
HOD 36:6-PC-/18:3	301824.8	122478.6	134239.1	61696.4	69821.4	32475.2	0.08978089	4.965
HOT 34:2-PC-/16:0	16493723	19311880	20449348	16124554	14757679	14744753	0.04842608	7.884
HOT 34:3-PC-/16:0	16770073	16078120	16163696	13224464	14821875	13685545	0.009686196	21.590
HOT 34:3-PG-/16:0	66058.394	80000	24239.13	54642.857	65178.571	69009.901	0.7389952	0.128
HOT 36:4-PC-/18:1	24306.569	25555.556	11847.826	53035.714	14107.143	16633.663	0.6100945	0.305
HOT 36:4-PC-/18:2	374890.5	550256.4	403260.9	479642.9	464196.4	567920.8	0.3884604	0.934
HOT 36:4-PG-/18:1	175328.47	196410.26	52608.696	51696.429	95089.286	92079.208	0.258402	1.733
HOT 36:5-PG-/oPDA 36:4 PG	21532.8	28119.7	5978.3	3125	5803.6	11287.1	0.1665093	2.852
HOT 36:6-PC-/18:3	48686.1	50000	47065.2	41160.7	29642.9	46138.6	0.1248379	3.751
HPOD keto 34:2-PC-/16:0	34817.5	111025.6	36847.8	52321.4	53035.7	59604	0.8259478	0.055
HPOD keto 34:2-PC-/16:0	172627.7	164188	222826.1	214196.4	224642.9	185049.5	0.381575	0.965
HPOD keto 34:2-PE-/16:0	75109.5	98717.9	65326.1	108839.3	98214.3	89901	0.1641181	2.894
HPOD keto 34:2-PG-/16:0	39416.1	43076.9	21847.8	54910.7	32053.6	36732.7	0.5370217	0.455
HPOD keto 34:3-PC-/16:0	6820073	6517350.4	5980000	5792142.9	5799910.7	6127425.7	0.1191336	3.911
HPOD keto 34:3-PC-/16:0	660802.9	655982.9	600760.9	519375	651517.9	619901	0.3937338	0.912
HPOD keto 34:3-PC-/18:3	2117226.3	2741880.3	4474565.2	4585982.1	893750	4329405.9	0.9143147	0.013
HPOD keto 34:3-PE-/HPOT keto 34:2-PE	627591.2	662735	574130.4	684642.9	671607.1	866336.6	0.1536639	3.089
HPOD keto 34:3-PG-/16:0	537591.24	621196.58	576847.83	649107.14	732589.29	841386.14	0.05535879	7.170
HPOD keto 36:4-PC-/18:1	2698686.1	1997948.7	2249891.3	2194375	2144642.9	2142079.2	0.4925564	0.569
HPOD keto 36:4-PC-/18:1	459416.1	482991.5	421739.1	447232.1	537946.4	525148.5	0.2193959	2.117
HPOD keto 36:4-PC-/18:2	1645985.4	1309743.6	1104565.2	1317500	1562410.7	302475.2	0.5212564	0.493
HPOD keto 36:4-PC-/18:2	262408.8	321709.4	255108.7	266696.4	328303.6	294059.4	0.5798696	0.362
HPOD keto 36:4-PE-/18:1	724671.5	889572.6	579565.2	953660.7	858660.7	1001782.2	0.1048355	4.368
HPOD keto 36:4-PE-/18:2	232992.7	253589.7	254782.6	232321.4	244553.6	221287.1	0.2139485	2.179
HPOD keto 36:4-PE-/18:3	138832.12	154786.32	113913.04	131696.43	153482.14	221683.17	0.3259398	1.251
HPOD keto 36:4-PG-/18:1	565328.47	751623.93	824673.91	907589.29	804017.86	981089.11	0.1186833	3.924
HPOD keto 36:4-PG-/18:2	153868.61	155128.21	189130.43	177500	191339.29	229801.98	0.1600161	2.968
HPOD keto 36:5-PC-/18:2	252700.7	283247.9	224782.6	190267.9	290178.6	221980.2	0.597846	0.327
HPOD keto 36:5-PC-/18:3	3274233.6	2904786.3	2831630.4	2606875	2870892.9	2522574.3	0.1227032	3.810
HPOD keto 36:5-PC-/18:3	24598.5	28461.5	20000	23928.6	19732.1	16336.6	0.2558532	1.755

HPOD keto 36:5-PE-/18:3	49927.007	57777.778	56956.522	80535.714	85892.857	85346.535	0.000651754	92.620
HPOD keto 36:5-PE-/HPOT keto 36:4 PE	254525.5	265384.6	203478.3	329553.6	233839.3	290891.1	0.265343	1.674
HPOD keto 36:5-PG-/18:2	259562.04	325982.91	254021.74	280892.86	320714.29	356732.67	0.28169	1.546
HPOD keto 36:6-PC-/18:3	947080.3	694871.8	864673.9	606339.3	794642.9	641683.2	0.1755711	2.702
HPOT keto 34:2-PC-/16:0	660802.9	655982.9	600760.9	519375	651517.9	619901	0.3937338	0.912
HPOT keto 34:2-PG-/16:0	526934.31	618632.48	576847.83	649107.14	735178.57	829801.98	0.04879957	7.841
HPOT keto 34:3-PC-/16:0	53047518	49862906	44425326	47274554	47361250	47897426	0.5604839	0.402
HPOT keto 34:3-PC-/16:0	117299.3	132307.7	78478.3	76071.4	110892.9	69703	0.3105298	1.346
HPOT keto 34:3-PE-/16:0	25839.416	28547.009	47934.783	39017.857	66607.143	53960.396	0.1456039	3.253
HPOT keto 34:3-PG-/16:0	151240.88	178034.19	220652.17	271875	266517.86	311980.2	0.01559205	16.330
HPOT keto 36:4-PC-/18:1	193795.6	193418.8	154239.1	156428.6	185982.1	188316.8	0.8405656	0.046
HPOT keto 36:4-PC-/18:2	3274233.6	2904786.3	1378804.3	1300000	1052053.6	1609405.9	0.1173185	3.964
HPOT keto 36:4-PE-/18:1	56861.314	53076.923	55869.565	48214.286	45535.714	37425.743	0.02829819	11.290
HPOT keto 36:4-PG-/18:1	261970.8	358888.89	328695.65	410625	380446.43	525445.54	0.08080388	5.400
HPOT keto 36:4-PG-/18:2	144452.55	310940.17	125326.09	176517.86	284821.43	258712.87	0.5285003	0.475
HPOT keto 36:5-PG-/18:2	35839.416	57521.368	42934.783	43928.571	56250	76336.634	0.3047591	1.383
HPOT keto 36:6-PC-/18:3	34525.5	48974.4	30108.7	75089.3	26517.9	7722.8	0.94878	0.005
LPC 13:0	49416.1	163675.2	314565.2	253839.3	229910.7	168118.8	0.6358375	0.262
LPC 14:0	8076642.3	4993162.4	14069457	12130714	12435268	8329207.9	0.5539772	0.416
LPC 15:0	746496.4	650170.9	1462826.1	807321.4	687678.6	702475.2	0.442365	0.725
LPC 16:0	14026788	10416923	20962717	19103304	20641339	15737129	0.3812535	0.966
LPC 16:1	39893796	28366752	63312174	60188661	51952946	39569307	0.6028051	0.318
LPC 18:0	1140583.9	729145.3	1611195.7	1083660.7	1394464.3	645643.6	0.7401258	0.126
LPC 18:1	39195839	26416581	60837391	58727232	50934464	37574257	0.588399	0.345
LPC 18:2	14800365	10596752	18063478	15727679	15956607	12186238	0.9587349	0.003
LPC 18:3	392700.7	422991.5	452391.3	496875	397946.4	394554.5	0.8599162	0.035
LPC 20:0	15401.5	25470.1	14565.2	24375	199821.4	8415.8	0.3906945	0.925
LPC 20:1	97153.3	23333.3	20326.1	75535.7	50178.6	68415.8	0.5352611	0.459
LPC 20:2	16569.3	9230.8	16847.8	13035.7	72500	14653.5	0.3857165	0.946
LPC 20:3	27956.2	28034.2	16521.7	17053.6	0	12178.2	0.08560258	5.159
LPC 20:5	5839.4	72649.6	21739.1	43839.3	17767.9	0	0.617779	0.292
LPC 22:1	20146	9658.1	34565.2	10892.9	16517.9	990.1	0.2324764	1.977
LPC 22:6	9635	16410.3	19891.3	6160.7	17857.1	23267.3	0.9427165	0.006
LPC 26:0	135328.5	96495.7	0	122767.9	92232.1	187920.8	0.3103567	1.347
LPC(O-16:0)	406204.4	106495.7	664021.7	753035.7	508839.3	401584.2	0.4451153	0.716
LPC(O-18:0	344744.5	134871.8	777065.2	766160.7	504196.4	179207.9	0.8127114	0.064
LPC(O-18:1)	344890.5	322051.3	674565.2	651428.6	573750	434752.5	0.461139	0.663
LPC(O-20:1)	145839.4	77692.3	196304.3	165892.9	243303.6	94257.4	0.6394144	0.256

LPC(O-24:2)	94379.6	58205.1	67608.7	64553.6	27232.1	43762.4	0.1388797	3.402
LPE(14:0))	1097737.2	777094	1574673.9	1436428.6	1166071.4	775445.5	0.9406096	0.006
LPE(16:0)	24217007	19993504	26377500	21817679	18649464	17911683	0.1413573	3.346
LPE(18:0)	3360438	2230769.2	3450869.6	1545357.1	2310000	2203663.4	0.09651274	4.681
LPE(18:1)	37572555	32011197	50273696	46774196	35402232	31949307	0.7989406	0.074
LPE(18:2)	5296277.4	4930341.9	6888587	5913125	4717589.3	4617524.8	0.4426274	0.725
M34:2-PC-/16:0	395180876	363748034	351048261	342870268	342812589	336958218	0.09316898	4.818
M34:2-PC-/16:0	394306.57	407094.02	522282.61	325982.14	387321.43	498514.85	0.5961013	0.331
M34:2-PC-/18:2	1160292	1162991.5	1193260.9	1130803.6	1363839.3	1273465.3	0.2889831	1.492
M34:2-PE-/16:0	428978.1	411452.99	599347.83	498035.71	554464.29	598217.82	0.3504465	1.116
M34:2-PE-/18:2	431970.8	490854.7	535434.78	558839.29	787232.14	649108.91	0.06995686	6.034
M34:2-PG-/16:0	87080.3	50598.3	86087	61428.6	64553.6	52970.3	0.2976693	1.431
M34:2-PG-/18:2	84525.5	75897.4	59456.5	64732.1	102589.3	69405.9	0.7088742	0.161
M34:3-PC-/16:0	205288248	179579316	164971304	144733661	158990714	144623366	0.05633544	7.081
M34:3-PE-/16:0	31751.825	14102.564	43260.87	13482.143	28482.143	30198.02	0.6023434	0.319
M36:4-PC-/18:1	39896058	35002821	33049022	23547321	28926875	26943960	0.02087534	13.670
M36:4-PC-/18:2	332481.75	404358.97	355434.78	268928.57	421785.71	346930.69	0.7287801	0.138
M36:4-PE-/18:2	489416.06	420000	553913.04	415535.71	515089.29	506930.69	0.8722579	0.029
M36:4-PG-/18:2	39708	70683.8	51304.3	40357.1	51160.7	25445.5	0.2719967	1.620
M36:5-PC-/18:3	2145036.5	1607948.7	1478695.7	977767.9	1344375	1143564.4	0.06260717	6.556
M36:6-PC-/18:3	26277.4	21453	5543.5	29553.6	5625	20198	0.9439353	0.006
modPC 540.5/0.78	92481.8	23418.8	154347.8	77678.6	115178.6	98415.8	0.8672662	0.032
modPC 666.4/1.90	46058.4	71282.1	126413	48928.6	130625	42970.3	0.8573074	0.037
modPC 843.6/7.10	3430.7	17265	20108.7	0	16607.1	39802	0.7017777	0.169
oddPC 29:0	10380073	9096923.1	10458044	7985625	8461696.4	7681980.2	0.01754043	15.210
oddPC 31:0	25436788	24147863	24158913	19602768	19123036	17848416	0.00106708	71.660
oddPC 31:1	66959489	67651880	65388370	53069643	53174732	48502970	0.000850249	80.680
oddPC 33:0	6205985.4	6853675.2	7004782.6	5535982.1	5872142.9	5309703	0.01929991	14.350
oddPC 33:1	66628613	67228889	62993696	52742857	52192143	51158515	0.000635075	93.880
oddPC 33:2	42559051	42484274	38779783	30696429	35250536	30897129	0.009766168	21.490
oddPC 33:3	4135255.5	3081453	3306304.3	2100803.6	2673214.3	2546237.6	0.0428324	8.582
oddPC 35:1	20165620	21617180	21501196	17508036	18260625	17546931	0.003213736	39.900
oddPC 35:3	7914817.5	8185128.2	7362500	4722678.6	5345089.3	5648811.9	0.002097904	50.160
oddPC 35:4	474233.6	471623.9	595543.5	295267.9	385625	328613.9	0.0218825	13.280
oddPC 35:5	112481.8	20427.4	53369.6	96785.7	19642.9	50594.1	0.8635523	0.034
oddPC 37:4	176350.4	205384.6	149239.1	124107.1	76517.9	93168.3	0.02088114	13.670
oddPC 37:6	93795.6	115641	150000	114732.1	211071.4	81485.1	0.7244094	0.143
oddPC 39:5	47591.2	30769.2	0	20357.1	8392.9	22673.3	0.5723056	0.377
oddPC 39:6	148613.1	95726.5	29673.9	69196.4	22232.1	62574.3	0.345093	1.144

oddPC 39:7	796496.4	665213.7	629347.8	590000	598750	735544.6	0.4673957	0.644
oPDA 34:2-PG-/16:0	48613.139	69743.59	24239.13	45625	65178.571	57623.762	0.5802333	0.361
oPDA 34:3-PC-/18:3	2557007.3	2462136.8	2601630.4	1867500	2110267.9	2009505	0.002615363	44.580
PC 26:0	9043576.6	8403247.9	9340543.5	7820267.9	6904196.4	7282574.3	0.01421074	17.260
PC 28:0	41012336	38012051	37600978	28233750	30338482	30657426	0.002270525	48.090
PC 30:0	49890511	48509658	48320435	40671875	41163036	40201188	0.000131507	210.300
PC 32:0	64124964	47951880	51744348	46508571	45863839	46619109	0.1657249	2.866
PC 32:1	1.096E+09	949320598	894489891	823483750	800763839	772320495	0.04326788	8.523
PC 32:2	714605766	759194103	686336957	619474018	587793929	578263564	0.007095336	25.780
PC 32:3	7523941.6	6919572.6	6176195.7	4118482.1	5242857.1	4881386.1	0.01420326	17.260
PC 34:0	39407080	29774872	29731848	26926607	26941161	23915446	0.1049374	4.364
PC 34:1	526784234	455642650	418366196	373336696	369518839	372850891	0.04049888	8.916
PC 34:2	722742263	662743419	590456739	536332054	546671161	524416139	0.03393236	10.030
PC 34:3	111489927	97736410	81599783	57655982	66711607	63167723	0.01889716	14.540
PC 34:4	16517445	12425128	12039022	8745357.1	10262679	8776138.6	0.04418801	8.401
PC 34:5	22481.8	79572.6	27500	19285.7	13125	19207.9	0.2301068	2.001
PC 36:0	4284744.5	3784273.5	3380760.9	3212767.9	2584464.3	3357128.7	0.09608195	4.698
PC 36:1	39466496	36233504	31654891	30757411	32092946	30801782	0.1189434	3.916
PC 36:2	208114891	182903077	166959674	149641339	139804018	149805644	0.03339886	10.140
PC 36:3	60267372	49016838	44360544	35052946	37733839	35523663	0.03442903	9.939
PC 36:4	111821752	81995385	71465109	46801161	56191964	57489505	0.0495952	7.753
PC 36:5	109263723	87146325	78250870	48961964	57864732	56272673	0.01805269	14.950
PC 36:6	168394.2	262393.2	85652.2	52410.7	58125	70594.1	0.09504217	4.740
PC 38:2	1659708	1375641	980543.5	673392.9	1054732.1	1000990.1	0.1358585	3.472
PC 38:3	193868.6	91025.6	146087	115178.6	247053.6	36930.7	0.8838343	0.024
PC 38:4	18686.1	22478.6	45760.9	0	5714.3	32475.2	0.2829759	1.536
PC 38:5	48175.2	31709.4	0	13125	15357.1	9405.9	0.3813321	0.966
PC 38:6	160948.9	104615.4	73913	338482.1	248928.6	281485.1	0.008455633	23.340
PC 38:7	287810.2	223418.8	296739.1	240982.1	212500	100297	0.1572595	3.020
PC 40:5	40583.9	20341.9	12500	28303.6	22500	19108.9	0.9004058	0.018
PC 40:6	45401.5	35299.1	30543.5	84464.3	47232.1	37821.8	0.2622913	1.700
PC 40:7	98467.2	96068.4	136739.1	81964.3	27053.6	199207.9	0.8906324	0.021
PC(O-32:2)	7722043.8	8168803.4	6812500	4728750	5706339.3	4507920.8	0.008879353	22.700
PC(O-34:4)	485839.4	265384.6	352065.2	259553.6	84732.1	150396	0.06847504	6.133
PC(O-36:0)	3907080.3	2801880.3	2993478.3	2106071.4	2392321.4	2437326.7	0.06084011	6.695
PC(O-36:2)	18313796	17914872	14745870	9512410.7	12060000	11010891	0.01046839	20.640
PC(P-30:0)	4440365	4291880.3	4975543.5	4104642.9	3714017.9	3886435.6	0.04763074	7.975
PC(P-36:5)	735109.5	575128.2	514782.6	696517.9	525892.9	510297	0.7463084	0.120
PE 32:0	17247956	17929487	16842717	14872946	14450714	15012178	0.00204525	50.840

PE 32:1	237484818	243279658	244171196	206988839	209591071	197340495	0.000980205	74.920
PE 34:0	43958759	41572137	46956413	35512679	35359375	37024257	0.007593431	24.810
PE 34:1	401046861	389968291	434603696	354046607	346661339	348633960	0.0124396	18.670
PE 34:2	346979051	334245214	380795217	297941250	290788571	292068119	0.01269138	18.450
PE 34:3	76113577	64712650	72089130	52336429	58277857	49321188	0.01420512	17.260
PE 35:1	12525256	12132992	15209565	9970803.6	11053125	11285941	0.07409138	5.776
PE 35:2	25839416	27483932	32513044	23332500	22913036	23436634	0.05557629	7.150
PE 36:0	5636861.3	4813076.9	5885652.2	4352321.4	4122589.3	4281089.1	0.02269401	12.980
PE 36:1	57491971	52846325	60681196	51065000	52192857	52151188	0.08687463	5.098
PE 36:2	157669051	159036154	181564891	145613214	142621071	153202970	0.08618244	5.131
PE 36:3	70605110	68882992	78503370	54173661	58903482	54501584	0.007259783	25.450
PE 36:4	20607299	18850513	20995326	12487946	13167054	14135050	0.001072643	71.470
PE 36:5	2020438	1528205.1	1512608.7	825892.9	940803.6	911881.2	0.009557675	21.760
PE 38:3	563649.6	759829.1	684347.8	500803.6	482767.9	472079.2	0.03329404	10.160
PE 38:4	24598.5	13846.2	23587	0	29732.1	16336.6	0.5961335	0.331
PE 40:7	37153.3	43846.2	14130.4	0	0	10099	0.04197704	8.701
PE(O-18:1/18:2)	9493868.6	7559401.7	11073152	8231339.3	7616785.7	7541089.1	0.2032972	2.308
PE(O-18:2/18:2)	41897.8	153418.8	193369.6	46517.9	52053.6	43168.3	0.1440109	3.288
PE(O-34:1)	8661386.9	8199914.5	10076630	7716964.3	8143839.3	6629306.9	0.1094467	4.211
PE(O-34:2)	6361678.8	5982649.6	7311739.1	4888125	5676071.4	4957425.7	0.04238376	8.644
PE(O-36:2)	27859562	29841624	34486087	23993929	24490000	24988317	0.03473333	9.881
PE(O-36:5)	19854	19914.5	41304.3	22053.6	13571.4	7425.7	0.2016655	2.329
PE(O-36:6)	832919.7	690427.4	813587	472053.6	636696.4	452277.2	0.02452114	12.370
PE(P-34:1)	6361678.8	5982649.6	7311739.1	4888125	5676071.4	4957425.7	0.04238376	8.644
PE(P-34:2)	76569.3	58717.9	24782.6	49017.9	9821.4	37722.8	0.3307738	1.223
PE(P-36:1)	25839416	27483932	32513044	23384196	22913036	23436634	0.05611401	7.101
PE(P-36:2)	9493868.6	7559401.7	11271957	8231339.3	7616785.7	7541089.1	0.2070589	2.262
PE(P-38:5)	140219	142820.5	68804.3	39107.1	81071.4	32178.2	0.08112035	5.383
PE(P-38:6)	4187372.3	3996495.7	4022608.7	3143839.3	3957767.9	3114455.4	0.07879739	5.507
PE(P-40:6)	2060802.9	2177777.8	1853587	1458750	1420892.9	1367227.7	0.00334377	39.050
PG 34:0	1762481.8	1901623.9	1815217.4	1444107.1	1196517.9	1467227.7	0.00878318	22.840
PG 34:1	12057226	10262821	9922717.4	8390625	7864732.1	8854851.5	0.03003732	10.870
PG 36:1	1354744.5	1532307.7	1240108.7	1013303.6	889285.7	860198	0.009422124	21.940
PG 36:2	7116569.3	6103418.8	5485652.2	5169732.1	3989821.4	4499009.9	0.04530112	8.258
PI 32:0	3993284.7	2875555.6	2184021.7	2248303.6	2382232.1	2093465.3	0.2194537	2.116
PI 32:1	40995183	36499573	28978370	28570179	24804107	25120990	0.06565587	6.329
PI 34:1	36341168	31234615	26673152	24915446	22990179	22066139	0.05005534	7.703
PI 36:2	33692117	27380427	23406087	21551518	21750982	20047723	0.08160964	5.358
PI 36:3	56620584	44548974	35233044	28327679	30646250	28564059	0.05926568	6.825

PI 36:4	9890365	8441709.4	6787282.6	5392321.4	6050625	4503861.4	0.03800073	9.307
PI 38:2	784890.5	634017.1	568152.2	567589.3	502232.1	575445.5	0.1702278	2.789
PI 38:3	363065.7	291111.1	267065.2	236339.3	274732.1	192475.2	0.1241131	3.771
PI 38:4	20656.9	23931.6	3260.9	35357.1	55982.1	47623.8	0.02580159	11.980
PI 38:5	13868.6	6923.1	1087	982.1	9375	990.1	0.4908351	0.574
PS 34:0	1448175.2	1458034.2	536413	427142.9	504910.7	264257.4	0.07541851	5.697
PS 36:1	19808832	15226667	4062282.6	4888660.7	5184910.7	4778514.9	0.1591018	2.985
PS 36:2	47652920	38141197	11469783	13370714	15620000	12785050	0.1638741	2.899
PS 38:3	353211.7	206581.2	0	62946.4	136339.3	52772.3	0.3870919	0.940
PS 38:4	33138.7	51111.1	26195.7	446.4	625	26237.6	0.07086002	5.976
TG 14:0 16:0 18:2	630494526	669751966	759477391	581729911	568705804	571942970	0.04279537	8.587
TG 14:0 16:1 18:1	535521898	549114444	615328696	479630625	465754107	510458119	0.04369724	8.466
TG 14:0 16:1 18:2	74904015	76900940	93190109	61805625	70173304	66145347	0.0675003	6.199
TG 14:0 18:0 18:1	59737883	66918974	35529348	58514554	22126339	22946436	0.270761	1.630
TG 14:0 18:2 18:2	230948.9	152906	236087	96607.1	241607.1	226930.7	0.7493702	0.117
TG 14:1 16:0 18:1	40544380	46924957	133421848	104736071	91062500	104773168	0.4301815	0.768
TG 14:1 16:1 18:0	1.567E+09	1.696E+09	1.83E+09	1.446E+09	1.34E+09	1.432E+09	0.02454911	12.360
TG 14:1 18:0 18:2	2523065.7	2262991.5	3556521.7	3186696.4	6131607.1	3363564.4	0.2337074	1.964
TG 14:1 18:1 18:1	32043.8	427350.4	108804.3	159285.7	18660.7	188019.8	0.6360887	0.261
TG 15:0 18:1 16:0	108613.1	0	8587	71875	51160.7	12475.2	0.8831162	0.025
TG 15:0 18:1 18:1	675401.5	627777.8	616087	445535.7	316785.7	491881.2	0.01613838	15.990
TG 16:0 16:0 16:0	97078540	109914957	114342283	103131071	88310625	80965248	0.1216602	3.839
TG 16:0 16:0 18:0	21970365	27405043	26078370	23567143	11130357	10018218	0.09184627	4.875
TG 16:0 16:0 18:1	3375036.5	4664957.3	4567282.6	2775892.9	3246339.3	3252277.2	0.06648643	6.270
TG 16:0 16:0 18:2	6980365	6661111.1	20597391	6279196.4	14378661	13268812	0.9851243	0.000
TG 16:0 16:1 18:1	5438394.2	6583418.8	6842608.7	5629375	5803392.9	6096039.6	0.3807717	0.968
TG 16:0 18:0 18:1	59024380	108557094	58420544	53022768	34311964	36052079	0.1246996	3.755
TG 16:0 18:1 18:1	4514671.5	5233162.4	5572173.9	4505714.3	4380446.4	6134059.4	0.8844064	0.024
TG 16:0 18:1 18:2	327445.3	400085.5	417717.4	302767.9	359464.3	305742.6	0.1497534	3.167
TG 16:0 18:2 18:2	164160.6	251623.9	122717.4	222232.1	170178.6	231386.1	0.5402058	0.447
TG 16:1 16:1 16:1	544308905	561594786	630601957	504186339	493976607	519528119	0.05619388	7.093
TG 16:1 16:1 18:0	28997226	31229145	42371739	28500625	29610982	35104158	0.5349839	0.460
TG 16:1 16:1 18:1	32561314	36603248	43274783	33790625	34746518	39146733	0.6768423	0.201
TG 16:1 18:1 18:1	35266423	35700855	49396413	36790893	38025000	47227525	0.9263327	0.010
TG 16:1 18:1 18:2	2711824.8	2434444.4	5661195.7	2660892.9	11846518	5588712.9	0.345706	1.141
TG 17:0 16:0 16:1	76938029	98935385	84180326	76551696	72030089	75574455	0.144803	3.271
TG 17:0 16:0 18:0	3445620.4	6447008.5	3920000	4506964.3	4204910.7	4150792.1	0.7526708	0.114
TG 17:0 17:0 17:0	3174671.5	4165470.1	2765326.1	3332321.4	3427321.4	3391584.2	0.9725453	0.001
TG 17:0 18:1 14:0	19571971	24934188	21418044	19981339	18069464	19664753	0.1787818	2.652

TG 17:0 18:1 16:0	12858248	18501709	15449239	12354107	19445179	14553069	0.9570205	0.003
TG 17:0 18:1 16:1	15497153	16956496	17988478	14367946	14165089	17637822	0.3470592	1.133
TG 17:0 18:1 18:1	855182.5	997435.9	820760.9	1189196.4	778214.3	940000	0.5841013	0.354
TG 17:0 18:2 16:0	27540073	32246325	28521630	24370089	24639643	26549505	0.05556407	7.151
TG 18:0 18:0 18:0	304525.5	271196.6	322173.9	317767.9	170446.4	338118.8	0.6863361	0.189
TG 18:0 18:0 18:1	1717080.3	3172222.2	1811195.7	3300892.9	2347857.1	1529108.9	0.8301572	0.052
TG 18:0 18:1 18:1	3664671.5	11226239	3179130.4	2476517.9	2002767.9	2120495	0.2166787	2.147
TG 18:0 18:2 18:2	40219	11282.1	34565.2	34642.9	18214.3	130792.1	0.4197964	0.807
TG 18:1 14:0 16:0	485358029	561037949	554505326	498236250	413928393	414283960	0.06900065	6.097
TG 18:1 18:1 18:1	250656.9	229658.1	290760.9	91250	199285.7	132079.2	0.03273679	10.270
TG 18:1 18:1 18:2	207518.2	96666.7	62500	49821.4	19285.7	224752.5	0.7698867	0.098
TG 18:1 18:2 18:2	2992.7	37179.5	10000	0	0	0	0.1839589	2.573
TG 48:0	46913942	52399915	47269674	39552500	33949732	33776139	0.007249388	25.470
TG 48:1	164514015	177732821	186932174	148161786	132334732	132367228	0.009802697	21.440
TG 48:2	80404599	76567350	85193261	63469911	61652500	67153366	0.005018251	31.270
TG 48:3	36990073	40431966	41958370	31656429	32390625	35573465	0.02559527	12.040
TG 49:1	6306934.3	5606068.4	6853804.3	5206964.3	5459910.7	6153168.3	0.2300537	2.002
TG 50:0	27762847	33635983	29193478	24392679	9178571.4	10506931	0.04013028	8.971
TG 50:1	106276204	115199915	61127609	93400000	40514286	43302079	0.2169026	2.145
TG 50:2	64464380	68555470	72122500	58767411	52781696	65158218	0.08714236	5.086
TG 50:3	20103723	20226239	23291739	18187768	17085268	20766535	0.1692936	2.805
TG 50:4	556934.3	1131880.3	1488804.3	910714.3	3175178.6	1605643.6	0.3107319	1.345
TG 51:0	952116.8	1751709.4	1355434.8	1456160.7	1380982.1	1535247.5	0.6800052	0.197
TG 51:2	4082408.8	3913247.9	4600434.8	2924642.9	3567500	4434455.4	0.3141488	1.323
TG 52:1	17029562	27634274	16381630	15477232	10756518	14801980	0.1652533	2.874
TG 52:2	18027226	19326068	22579565	15288304	7028482.1	19112772	0.1811814	2.615
TG 52:4	233941.6	283418.8	284565.2	222410.7	827232.1	382376.2	0.3120675	1.336
TG 53:2	16276350	28321111	18355544	14912321	15642679	17134555	0.2489284	1.817
TG 54:1	594087.6	828974.4	395652.2	621785.7	68928.6	100891.1	0.1924001	2.452
TG 54:2	9854	35299.1	7500	37857.1	14821.4	19207.9	0.6026968	0.318
TG 54:3	1263211.7	1341025.6	1254456.5	1124285.7	1370535.7	1770198	0.5157417	0.507
TG 54:4	276204.4	135213.7	39565.2	274107.1	339821.4	200099	0.2035415	2.305
TG 54:5	172627.7	133589.7	86630.4	51160.7	93482.1	46039.6	0.0811771	5.380
TG 54:6	199124.1	232051.3	338587	206250	203660.7	211782.2	0.3066598	1.371
TG 56:6	76715.3	142649.6	244347.8	86071.4	9107.1	136930.7	0.2763682	1.586
TG 56:8	518978.1	423589.7	645108.7	423482.1	379107.1	515940.6	0.3019053	1.402

1189

1190

1191